Sapienza Università di Roma

Department of Information Engineering, Electronics and Telecommunications

Ph.D.in Information and Communication Technology – XXX Cycle

Estimating the Concentration of Physico-Chemical Parameters in Hydroelectric Power Plant Reservoir

Candidate
Hieda Adriana Nascimento Silva

Thesis Advisor
Prof. Massimo Panella

Co-Advisor
Prof. Rita Asquini

Thesis not yet defended

Estimating the Concentration of Physico-Chemical Parameters in Hydroelectric Power Plant Reservoir

Ph.D. thesis. Sapienza – University of Rome
ISBN: 000000000-0

This thesis has been typeset by LaTeX and the Sapthesis class.

Version: October 31, 2017

Author's email: hiedans@gmail.com

Dedicated to
My mom

Abstract

The United Nations Educational, Scientific and Cultural Organization (UNESCO) defines the Amazon region and adjacent areas, such as the Pantanal, as world heritage territories, since they possess unique flora and fauna and great biodiversity. Unfortunately, these regions have, increasingly, been suffering from anthropogenic impacts. One of the main anthropogenic impacts in the last decades has been the construction of hydroelectric power plants.

As a result, dramatic altering of these ecosystems has been observed, including changes in water levels, decreased oxygenation and loss of downstream organic matter, with consequent intense land use and population influxes after the filling and operation of these reservoirs. These, in turn, lead to extreme loss of diversity in these areas, due to large-scale deforestation. The fishing industry in place before construction of dams and reservoirs, for example, has become much more intense, attracting large populations in search of work, employment and income.

Environmental monitoring is fundamental for reservoir management, and several studies around the world have been performed in order to evaluate the water quality of these ecosystems. The Brazilian Amazon, in particular, goes through well defined annual hydrological cycles, which are very importante since their study aids in monitoring anthropogenic environmental impacts and can lead to policy- and decision-making with regard to environmental management of this area. The water quality of Amazon reservoirs is greatly influenced by this defined hydrological cycle, which, in turn, causes variations of microbiological, physical and chemical characteristics.

Eutrophication, one of the main processes leading to water deterioration in lentic environments, is mostly caused by anthropogenic activities, such as the releases of industrial and domestic effluents into water bodies. Physico-chemical water parameters typically related to eutrophication are, among others, chlorophyll-a levels, water transparency and total suspended solids, which can, thus, be used to assess the eutrophic state of water bodies

Usually, these parameters must be investigated by going out to the field and manually measuring water transparency with the use of a Secchi disk, and taking water samples to the laboratory in order to obtain chlorophyll-a and total suspended solid concentrations. These processes are time- consuming and require trained personnel. However, we have proposed other techniques to environmental monitoring studies which do not require fieldwork, such as remote sensing and computational intelligence.

Simulations on different sample station of the study area were performed to determine a relationship between these physico-chemical parameters and the spectral response of the reservoir. Based on the in situ measurements, empirical models were established in order to relate the reservoir reflectance measured by Landsat 7 Enhanced TM+ with the water optical parameters for Tucurui reservoir. Four images for each year from 2007 to 2014 were calibrated and atmospherically corrected.

Statistical analysis using error estimation was employed, aiming to evaluate the most accurate methodology. The ANN are trained by hydrological cycle, considered full, emptying, dry and filling and are shown to be useful in estimating the physico-

chemical parameters of water from reflectance of visible and NIR bands of satellite images, with better results for the period with little rain and few clouds in the analyzed region.

Contents

Nomenclature

$(\mu s/cm)$ Microsiemens per centimeter

(Chl_a) Chlorophyll Concentrations

(mg/lit) Milligram per liters

$(NH4_4^+ - N)$ ammonium

$(NO2_2^- - N)$ nitrite

$(NO3_3^- - N)$ nitrate

$(PO4_4^{3-} - P)$ soluble phosphate

$ANFIS$ Adaptive Neuro Fuzzy Inference System

ANN Artificial Neural Network

BOD Biochemical Oxygen Demand

BP Back Propagation

BPA Back Propagation Algorithm

COD Chemical Oxygen Demand

$COSQC$ Central Organization for Standardization and Quality Control

Cr Chromium element

CWT Continuous Wavelet Transform

DNs Digital Numbers

DO Dissolved oxygen

DOS Dark Object Subtraction

EC electrical conductivity

$FBNN$ Feedforward Neural Network

Fe Iron element

FIS Fuzzy Inference System

MLP Multi layer perceptron

$MLPANN$ Multi-Layer Rerceptron Articial Neural Network

MSE Mean Squared Error

$NERC$ Natural Environment Research Council

R River

Rrs Remote Sensing Reflectances

SCP Semi-automatic Classification Plugin

SD Secchi Disk Depths

SVM Support Vector Machine

TDS Total Dissolved Solids

TDS total dissolved solids

$Temp$ Temperature

TN Total Nitrogen

TP Total Phosphorus

TS total solids

TSS Total Suspended Solids

TUR turbidity

$USGS$ United States Geological Survey

WB Waterbody

WNN Wavelet Neural Network

WT Wavelet

Zn Zinc element

PCPC Physico-Chemical Parameters Concentrations

Chapter 1

Introduction

In this chapter I will discuss the justification, importance of Research and motivation and general search context of thesis.

I will describe the aims, etc...

1.1 Justification - Importance of Research and motivation

Water is one of the most essential components of human life. This natural resource generates socioeconomic development for society in general, more specifically for industry, agriculture and public use. Water quality involves physico-chemical and biological processes. These processes are necessary for the existence of life as it is an important factor for health. Therefore, the monitoring of water quality variables is of fundamental importance for society in general.

The values of the physico-chemical parameters present in the water should be within the standards allowed by the legislation, since the presence of components in high concentrations can be harmful to human health and the ecosystem. However, the presence of these components in the Water is important for the geochemical cycle and environmental health, so it is necessary to analyze and periodically monitor these components[1].

Due to the development and economic and population growth, Brazil is increasingly constructing water reservoirs, thus increasing the demand for drinking water and hydroelectric potential. [2]

Water reservoirs have different seasonal characteristics and several studies have been developed to identify and characterize seasonal differences as well as physico-chemical parameters in aquatic environments.[3] [4]

Some researches were developed with the objective of identifying physico-chemical parameters in aquatic environments using Computational intelligence [5] [6] [7] [8]. However, these studies do not analyze the hydrological cycles of the regions.

In this context, this research proposes a method, using the techniques of computational intelligence to infer levels of the physico-chemical parameters in bodies of water in reservoirs, using historical data, collecting water several years, analyzing and predicting the physico-chemical parameters per hydrological cycle.

In this sense, this project aims to investigate and propose a computational solution, using computational intelligence and remote sensing techniques to infer the levels of physico-chemical parameters present in the body of water.

Satellite images were used, captured in the same period of the water collection, verified the reflectance of the substances in the images, so we developed a neural network to predict these parameters.

In the study we intend to investigate the reflectance condition in water bodies of two reservoirs, one in the Brazilian Amazon, considered a deep reservoir (reservoir of the hydroelectric plant of Tucuruí) and another located in the United Kingdom, Cefni, in order to validate the proposed model.

1.2 Context of research - Contextualization, conceptualisation

The construction of hydroelectric power plants in the Amazon region has generated social and environmental impacts in the last decades [9], and statistical data indicate that renewable energy, including hydroelectric power, is expected to increase by almost 85% between now and 2030. [10].

While Russia and China have natural gas and coal reserves, Brazil relies on hydro power for 85% of its electricity needs [11].

The changes in the aquatic environment due to the construction of reservoirs have been studied by several authors[12][13]. And these studies have shown that the changes in physico-chemical parameters can directly affect water quality and local biota because freshwater ecosystems are an important natural resource, essential for multiple purposes such as drinking, domestic use, industrial cooling, power generation, agriculture, waste disposal, and transportation routes.[14].

The presence of physico-chemical parameters in waterbody is also an important component for the geochemical cycle and biodiversity, but high concentrations can negatively influence ecosystems when they are in quantities not allowed by legislation[5] [15] [16]. For these reasons, many scientists have studied the influence of physico-chemical parameters in freshwater and how this affects ecosystems.

Studies involving Remote Sensing, Artificial Neural Networks (ANN), Wavelet Transform, Adaptive neuro-fuzzy inference systems (ANFIS) with cross-validation and Statistical Analysis have recently gained attention in the literature for the monitoring of water quality. [17] [18] [19] [20] [21] [22][23] [24][25][26][27][28] [29] Among the monitoring techniques used are those using remote sensing [30]and computational intelligence [31].

The artificial neural network (ANN) technique is a tool for modeling real-world problems and has been used to evaluate the physico-chemical parameters of water cite sarkar2015river, cite samarasinghe2016neural.

Another technique that has also been gaining attention in prediction models for water quality monitoring is the adaptive neuro-diffuse inference system (ANFIS) [32]. In some studies, the performance of the ANFIS model was compared with an artificial neural network model. The ANFIS model was able to provide greater accuracy, particularly in the case of extreme events [19]. Considered an option with greater precision and reliability for the treatment of forecasting problems involving training and prediction of concentrations of various parameters.

Among the evaluated parameters, we can mention: Chlorophyll Levels (C), Total Suspended Solids (TSS) and Transparency (T), these parameters can influence the ecosystems and were considered important factors for monitoring water quality in reservoirs[33][34] [35] [36].

All these parameters are currently evaluated, however, the methods currently used for water analysis are very time-consuming, extremely expensive because they require sample collection, trained personnel and specialized laboratories.

We propose a less expensive and more dynamic method to monitor these parameters, using techniques of artificial intelligence and remote sensing.

The proposed method uses satellite images and the "in situ" measurements made by the responsible companies. The water samples were collected in 7 sampling stations called: Caraipé 1 (C1), Caraipé 2 (C2), Breu Branco (MBB), Jacunda (MJV), Upstrem 1 (M1) Upstrem 3 (M3), Ipixuna (MIP).

The Satellite Sensor chosen was Landsat 7 ETM +, which has a spatial resolution of 30 m for the six reflective bands, 60 m for the thermal band, and includes a panchromatic band (pan) with a resolution of 15 m.

Landsat 7 has a 378 gigabit(Gb) Solid State Recorder (SSR) that can hold 42 min (approximately 100 scenes) of sensor data and 29 h of housekeeping telemetry concurrently (L7 Science Data User's Handbook[1]).

We downloaded the satellite images of 2007, 2008, 2009, 2010, 2011, 2012, 2013 and 2014 from the Earth Explorer USGS [2]. These images were classified and converted into vector format, which served as inputs for the neural model. The output of the neural network was validated with the samples analyzed in a chemical laboratory performed by the companies responsible.

The ANFIS Wavelet technique was developed to monitor the physico-chemical parameters. Leave-One-Out Cross Validation was used to validate the model tested in two reservoirs: Tucurui and Cefni.

[1] http://landsathandbook.gsfc.nasa.gov/handbook.html
[2] https://espa.cr.usgs.gov/

1.3 Objectives

The degradation of surface water quality occurs due to the presence of various types of pollutants generated from human, agricultural, and industrial activities. Thus, mapping concentrations of different surface water quality parameters (SWQPs), such as turbidity, total suspended solids (TSS), chemical oxygen demand (COD), biological oxygen demand (BOD), and dissolved oxygen (DO), is indeed critical for providing the appropriate treatment to the affected waterbodies.

Traditionally, concentrations of SWQPs have been measured through intensive field work. Additionally, quite a lot of studies have attempted to retrieve concentrations of SWQPs from satellite images using regression-based methods.

However, the relationship between SWQPs and satellite data is complex to be modelled accurately by using regression-based methods. Therefore, our study attempts to develop an artificial intelligence modelling method for mapping concentrations of both optical and non-optical SWQPs.

In this context, a remote-sensing framework based on the back-propagation neural network (BPNN) is developed to quantify concentrations of different SWQPs from the Landsat7 ETM+ satellite imagery.

Compared to other methods, such as Support Vector Machine, significant coefficients of determination (R2) between the Landsat7 surface reflectance and concentrations of SWQPs were obtained using the developed Landsat7-based-BPNN models.

This research has the following general objective and specific objectives:

1.3.1 General objective

This project aims to develop computational solutions based on computer intelligence paradigms to aid in the monitoring of water bodies in reservoirs. In this sense, this proposal aims at the creation of computational solutions with remote sensing and wavelet neural networks to analyze the reflectances of the satellite images and to estimate the physico-chemical parameters concentrations present in the waterbody. The goal is to create an artificial neural model to predict the parameters and infer the future level of these substances.

1.3.2 Specific objectives

- Search for reflectance in the images and physico-chemical parameters in water bodies of the reservoirs.
- Analyze the available historical data base of the physico-chemical parameters.
- Analyze the satellite images corresponding to the dates of the water samples collected by the responsible company.
- Develop a neural model using Computational Intelligence techniques and satellite imagery to monitor current collection points.
- Use data mining techniques to identify patterns of behavior in historical data series.
- Propose a solution, low cost, using Computational Intelligence techniques to infer levels of physico-chemical parameters present in the reservoirs water bodies,

where the reflectance conditions manifest favorable to infer the future level of these substances, from reservoir images.

- To evaluate and propose the repositioning of the water sampling points of the Tucurui hydroelectric reservoir through the interpretation of satellite images of these reservoirs using paradigms of Computational Intelligence techniques, classification, Clustering and Statistical Analysis
- To contribute to the debate on the issues investigated, presenting proposals for contemporary solutions.

1.4 Problematic or Issue

- The growing energy demand results in the implementation of several hydropower plants in the last decades.

- Need to monitor the variables of water quality..

- Physico-chemical parameters concentrations should comply with standards established by environmental legislation.

1.5 Methodology

We studied physico-chemical parameters present in the water reservoir from 2007 to 2014. We applied a Neural Network Wavelet to infer the future levels of these concentrations in two reservoirs. We then used statistics models to validate the results.

- Use computational intelligence and remote sensing techniques to monitor physico-chemical parameters considering the hydrological cycle of the study area.

The analyzed study area, Tucurui, has 4 hydrological cycles: Full, Emptying, Empty, Filling as follows:

Full (March, April and May) Emptying (June, July and August) Empty (September, October , November) Filling (December, January, February)

Physico-chemical parameters Monitored:

Temperature (oC)
Secchi disk (m)
Conductivity (µS/cm)
pH
STS (mg / L)
Ammonia (mg / L)
NO3 (mg / L)
Chlorophyll (mg / L)
Turbidity (NTU)
dissolved oxygen (mg / L)
PO4 (mg / L)
P Total (mg / L).

The methodology used involves water collecting, satellite images from Landsat 7, ANN and LOO as explained in the following:

1.5.1 Water collection

The water data were provided by the Eletronorte/Eletrobras Company and the points chosen are considered the most important by this company for water analysis. These data were collected from January 2007 to December 2014. The relationship between Chlorophyll-a Levels, Total Suspended Solids, Transparency and spectral response of the riverwater was determined using the physico-chemical water samples collected. These data have been extracted from the samples and analyzed. We compared it to the proposed parameters level extracted from the remote sensing images, analyzed with an ANN method, described below. This was done for the entire hydrological cycle of the area.

1.5.2 Satellite Images

Thirty two satellite images from Landsat 7, sensor ETM+ were acquired. In order to obtain directly the TSS, C and T concentration from the reflectance of the satellite images, all satellite-image bands from visible and NIR were first calibrated for radiance values and, subsequently, for reflectance values. Image-based methods for atmospheric correction can estimate path radiance without using atmospheric properties, their accuracy is highly dependent on what is captured in a scene, as described in many papers: [37], [38], [39], [40], [41]. The characteristics of the analyzed bands are reported in table 1.1

Table 1.1. Characteristics of Visible and NIR Bands of the Analyzed Sensors

Satellite	Bands	Spectral Resolution(nm)	Spatial Resolution(m)	Temporal Resolution
Landsat7(ETM+)	TM1	450-520	30	16 days
Landsat7(ETM+)	TM2	520-600	30	16 days
Landsat7(ETM+)	TM3	630-690	30	16 days
Landsat7(ETM+)	TM4	760-900	30	16 days

The proposed method corrects the atmospheric effect by estimating the path radiance spectrum based on the dark object subtraction (DOS) method so that the spectrum meets general spectral characteristics of path radiance. The atmospheric effects that influence the signal registered by remote sensors might be minimized in order to provide reliable spectral information.

In aquatic systems, the application of atmospheric correction avoids the under or overestimation of remote sensing reflectance (Rrs). Accurately Rrs provides better information about the state of aquatic system establishing the concentration of aquatic compounds more precisely [42].

In this study, the DOS method with semi-automatic classification plugin was used, as described elsewhere [43][44]. Afterwards, a relative scattering model was chosen based on the atmospheric conditions of the image at the acquisition time and the initial haze value for the other spectral bands were then calculated.

Equations and parameters to convert calibrated Digital Numbers (DNs) to physical units, such as at-sensor radiance and reflectance, have been presented in a “sensor-specific” manner elsewhere [45].

DN to Radiance: There are two formulas that can be used to convert DNs to radiance; the method you use depends on the scene calibration data available in the header file(s). One method uses the Gain and Bias (or Offset) values from the header file. The longer method uses the LMin and LMax spectral radiance scaling factors.

Conversion to spectral radiance is a substantial improvement over use of DNs in analysis. When transformed, all individual sensor measurements are in comparable physical units. This is generally accomplished through information supplied by the instrument developer in the form [46],[47] :

$$rad_\lambda = LMIN_\lambda + (Q_{cal} - Q_{calmin}) \left(\frac{LMAX_\lambda - LMIN_\lambda}{Q_{calmax} - Q_{cmin}} \right), \tag{1.1}$$

$$ref_{i,j} = CH_{i,j} \times GAIN\_BAND + OFFSET\_BAND. \tag{1.2}$$

where:
Lλ: Spectral radiance at the sensor's aperture $[W/(m^2 \times sr \times \mu m)]$
Qcal: Quantized calibrated pixel value [DN]
Qcalmin: Minimum quantized calibrated pixel value corresponding to LMINλ[DN]
Qcalmax: Maximum quantized calibrated pixel value corresponding to LMAXλ[DN]
LMINλ: Spectral at-sensor radiance that is scaled to Qcalmin $[W/(m^2 \times sr \times \mu m)]$
LMAXλ: Spectral at-sensor radiance that is scaled to Qcalmax $[W/(m^2 \times sr \times \mu m)]$
GAIN_BAND: Band-specific rescaling gain factor $[(W/(m^2 \times sr \times \mu m))/DN]$
Brescale: Band-specific rescaling bias factor $[W/(m^2 \times sr \times \mu m)]$
ESUN: Mean exoatmospheric solea irradiance
SEA: Sun elevation
SZA: 90.0 - SEA
OFFSET_BAND: The DN value where zero radiance is detected 1.2

Table 1.2. ETM+ spectral radiance range $(W/m^2 - sr - \mu m)$

Band Number	Low gain		High gain	
	LMIN	LMAX	LMIN	LMAX
1	- 6.2	293.7	-6.2	191.6
2	-6.4	300.9	-6.4	196.5
3	-5.0	234.4	-5.0	152.9
4	-5.1	241.1	-5.1	157.4

A group of thirty two (32) satellite images were acquired from Landsat ETM+ in the same period of collection of water made on situ. Images from 2007 to 2013 were used to train the system while the images from 2014 was used to validate the methodology.The images acquisition date are presented in table 1.3

1.5.3 ANN and LOO

An ANN is a parallel-distributed processor that resembles the human brain by acquiring knowledge through a learning process and, then, stores the knowledge in the connection strength between computational units called neurons[48]. We used for this purpose a simple feedforward neural network in which the information moves

Table 1.3. Images used for Training and Validation

Training							Validation
2007	2008	2009	2010	2011	2012	2013	2014
07-MAY	09-MAY	12-MAY	15-MAY	02-MAY	04-MAY	23-MAY	26-MAY
11-AUG	13-AUG	16-AUG	19-AUG	22-AUG	24-AUG	11-AUG	14-AUG
15-NOV	01-NOV	20-NOV	07-NOV	10-NOV	12-NOV	15-NOV	02-NOV
15-JAN	18-JAN	20-JAN	23-JAN	10-JAN	13-JAN	31-JAN	18-JAN

in only one direction, from the input to the output nodes. The preprocessed data is given as the input of the ANN, and the outputs are: C, S and T. We used the Leave-One-Out (LOO) method to partition the dataset into training (Tr) and test set (Ts). We split the data set D of size N into N partitions of size 1 such that:

$$D = Q_1 \cup Q_1 \cup ... \cup Q_{N-1} \cup Q_N \tag{1.3}$$

with $Q_i \cap Q_j = 0$ for $i \neq j$. Each partition Q_i is used systematically for testing exactly once whereas the remaining partitions are used for training. Let $P_i = D - Q_i$ be the training set with respect to the test partition Q_i with $i = 1, ..., N$, then we can compute the error for each test partition for the trained model. The average error over all partitions is considered as the LOO Error. The reported result is the one with the least LOO Error in the test.

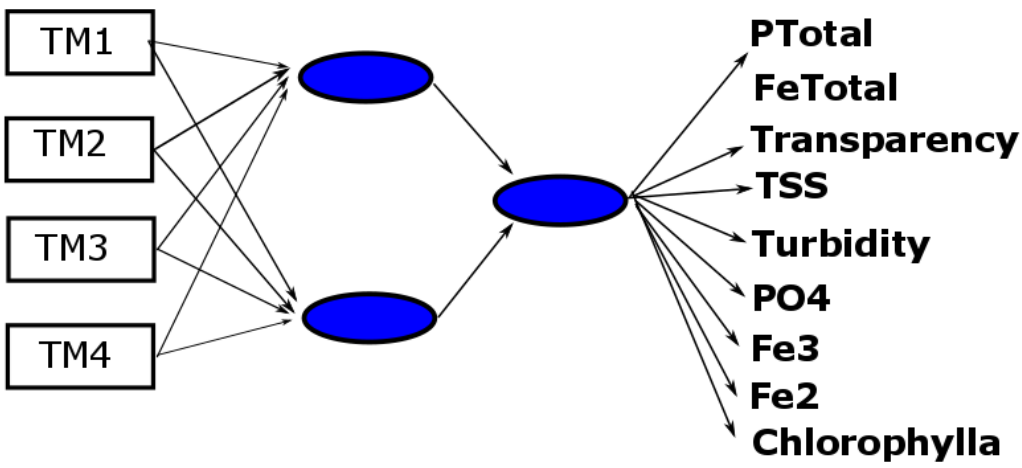

Figure 1.1. ANN Model by TM

The Fig 1.1 shows Inputs for the neural network from image landsat satellite, sensor ETM, band 1, band 2, band 3 and band 4. The process was repeated for each year from 2007 to 2014. As a result, estimates for chlorophyll a (C), Transparency (T) and Total Suspended Solids (TSS).

Chapter 2

State of the Art

Several researches have been done to identify and characterize seasonal variations of physico-chemical parameters in aquatic environments. Among the most used techniques are: ANFIS, multivariate analysis and artificial intelligence techniques.

Recently, the artificial neural networks have been examined for similar prediction applications and showed great potential to tackle and detect its nonlinearity behavior. According to the author [49]Heavy metal toxicity is a matter of considerable concern for environmental researchers. A highly cause of heavy metal toxicity in the aquatic environments is considered a serious issue that required full attention to understand in order to solve it. Heavy metal accumulation is a vital parameter for studying the water quality. Therefore, there is a need to develop an accurate prediction model for heavy metal accumulation. The author developed a model radial basis function neural network algorithm to investigate and mimic the relationship of heavy metals with the climatic and pollution conditions in lake water bodies.

The model was implemented in different climatic conditions as well as polluted and non-polluted lakes. Weekly records of physico-chemical data parameters (e.g., PH, EC, WT, DO, TDS, TSS, CL, NO3, PO4 and SO4) and Climatic parameters (e.g., air temperature, humidity And rainfall) were used as input data for the modeling, whereas the heavy metal concentration was the output of the model. Three different scenarios for modeling the input architecture considering the climate, pollution or both Have been investigated and the results obtained from all the scenarios are positively encouraging with high-performance Accuracy. Furthermore, the results showed that Isolated model for each condition achieves a better prediction Accuracy level rather than developing one general Model for all conditions.

The author [50] determined ecological stream health (ESH) and analyze trophic relations of nutrients (N, P) − chlorophyll and macroinvertebrate − fish, which is associated with stream morphology, land-use patterns, and water chemistry. The neural network modeling of a self-organizing map (SOM) suggested that clustering of trained SOM units reflected stream morphology, land-use patterns, and water chemistry, which influenced community structures and tolerances of top trophic level fish species in the ecosystem. Lotic ecosystem health, based on a multi-metric approach (MF-IBI model), was clearly demonstrated by a multivariate analysis (PCA); important factors were watershed characteristics (land-use patterns), nutrient levels (N, P), organic matter (BOD, COD) regimes, and biological components (trophic and tolerance guilds). In the research [51] twenty-five water quality parameters, including eight heavy metals, were studied at four sampling sites over a stretch of 63 km between Beas and Harike towns for pre-monsoon, post-monsoon and winter seasons. Artificial neural network models were fitted to the data. Correlations between the target values from ANN for turbidity, Biochemical Oxygen Demand (BOD)and bands 2 (green), 3 (red) and 4 (near infra-red) were highly significant.

The degradation of water quality is a major problem worldwide and often leads to serious environmental impacts and concerns about public health [52]. The water quality monitoring and assessmen of the Lakes has been done by many authors as following:

In the Koumoundourou Lake, a brackish urban shallow lake located in the northeastern part of Elefsis Bay (Greece), were evaluated. A number of water quality parameters (pH, temperature, dissolved oxygen concentration, electrical conductivity, turbidity, nutrients, and chlorophylla concentration) were analyzed in water samples collected bimonthly over a 1-year period from five stations throughout the lake. Statistical analysis was performed in order to evaluate the water quality of the lake and distinguish sources of variation measured in the samples. Satellite images of Landsat 5 Thematic Mapper were used in order for algorithms to be developed and calculate the concentration of chlorophyll-a (Chl-a). The trophic status of the lake was characterized as oligotrophic based on phosphorus and as mesotrophic–eutrophic based on Chl-a concentrations. The results of the remote sensing application indicated a relatively high coefficient of determination (R2) among point sampling results and the remotely sensed data, which implies that the selected algorithm is reliable and could be used for the monitoring of Chl-a concentration in the particular water body when no field data are available[52].

In binh dai ben tre, Vietnam, Monitoring surface water quality was also one of the essential missions especially in the context of increasing freshwater demands and loads of wastewater fluxes. The method of Fault Movement Potential (FMP) was used to assess the Surface water resources played a fundamental role in sustainable development of agriculture and aquaculture. Recently, remote sensing technology has been widely applied in monitoring and mapping water quality at a regional scale replacing traditional field-based approaches. This study assessed the application of the Landsat 8 (OLI) images for estimating Chemical Oxygen Demand (COD) as well as detecting spatial changes of the COD concentration in river reaches of the Binh Dai district, Ben Tre province, a downstream area of the delta. The results applied the Artificial Neuron Network (ANN) approach. [53]

A model that predicts the monthly water quality for a reservoir was constructed based on a newly developed programming system, the genetic algorithm operation tree (GAOT) was recently proposed. GAOT, which consists of genetic algorithm (GA) and operation tree (OT), is to find the best function, and to explore complex relationships between inputs and outputs when physical models cannot be defined in advance. In this study, was applied GAOT to estimate the total phosphorous (TP) in Feitsui Reservoir of Taiwan. From GAOT, the three significant input variables was extracted from 15 input variables, including the TP concentration of the Diyu Creek tributary, the TP concentration of main inflow Peishih Creek, the maximum rainfall in the watershed and TP concentration in reservoir, and expressed them appropriately in a sophisticated mathematical manner with accepted complexity.

The sensitivity analyses reconfirm the effectiveness of the selected variables in the nonlinear mathematical equations [54].

Another research worked issues inherent to the design of navigation planning and control systems required for adaptive monitoring of pollutants in inland waters. Proposed a new system for estimating water quality, in particular the chlorophyll-A concentration, by using satellite remote sensing data. The aim was to develop an intelligent model based on supervised learning, with the goal of improving the precision of the evaluation of chlorophyll-A concentration. To achieve this, an intelligent system based on statistical learning was used to Classify the waters a priori, before estimating the chlorophyll-A concentration with neural network models. therefore, was developed several models for the same surface of water, based on the spectral signature of the samples acquired in-situ. A control architecture was proposed to guide the trajectory of an aquatic platform to collect in-situ measurements It uses a multi-model classification/regression system to determine and forecast the spatial distribution of chlorophyll-A. Experimental results were presented to validate the approach using data collected on Lake Winnipeg in Canada[55] .

Remote-sensing framework based on the back-propagation neural network (BPNN) also wass developed to quantify concentrations of different surface water quality parameters (SWQPs) from the Landsat8 satellite imagery. Estimating turbidity, total suspended solids (TSS), chemical oxygen demand (COD), biological oxygen demand (BOD), and dissolved oxygen (DO), Considering the mapping concentrations of different SWQPs critical for providing the appropriate treatment to the affected waterbodies. [56]

In the Albufera de Valencia, Spain, also was develop an integrated algorithm for data fusion and mining of satellite remote sensing images to generate daily estimates of some water quality parameters of interest, such as chlorophyll a concentrations and water transparency, showed that the spatiotemporal variations of water transparency and chlorophyll a concentrations may be assessed simultaneously on a daily basis throughout the lake for environmental management using a genetic programming (GP) models[57].

Although these studies demonstrate the application of artificial intelligence and remote sensing to water quality monitoring, none of these studies addresses the application of this technique to water quality monitoring considering the regional hydrological cycle, seasonally, mainly in Amazon reservoirs where Cycle changes four times a year. Thus, this research becomes a pioneer in the application of artificial intelligence and the monitoring of water quality in reservoirs through remote sensing images, training the Neural Network Wavelet by hydrological cycle, that is, a network for each cycle, demonstrating that it is possible to achieve the objective of the research using these techniques.

Chlorophyll_a, TSS and Transparency have evaluated in this research in this research.Chlorophyll-a is an important constitutent reflecting both water quality status and ecosystem state because it is required for phytoplankton existence and can be considered an indicator of algal growth or an indirect indicator of nutrients [58]. Excessive growth of algae blooms in oceans and coastal areas decreases the amount of dissolved oxygen and causes eutrophication in rivers and streams. Because measuring chlorophyll-a is relatively simpler than algae biomass, chlorophyll-a is more often used as a trophic indicator[59].

Chlorophyll-a measurement is costly and time consuming, but remote sensing can provide a spatial view and long term trend of this parameter. Reflectance of chlorophyll-a concentration varies between blue and green sections. In other words, a higher concentration of chlorophyll-a increases reflectance in blue wavelengths and increases the reflectance in green wavelengths[60].

Dissolved organic matter (except phytoplankton) in the water as well as chlorophyll-a concentration can affect this ratio, however; radiation is highly absorbed by chlorophyll-a at about 450 and 670 nm[60][61] concluded that the peak reflectance of different concentrations of chlorophyll-a in a lake is about 700 nm wavelength. Most empirical ocean color algorithms for determining chlorophyll-a concentration are based on the correlations between chlorophyll-a concentration and spectral blue-to-green upward spectral radiance.

Maximum absorption of chlorophyll-a occurs in the blue waveband located in the maximum phytoplankton absorption (440 nm); however, the minimum phytoplankton absorption (550–555 nm) occurs in the green waveband [62]. Uncertainties may occur in determining chlorophyll-a concentration during cyanobacteria blooms[63] or in monitoring surface water with high suspended sediment concentration. In eithor case above, the conventional blue-green ratio is less applicable because the blue light signal decreases with increasing chlorophyll-a concentration. The fluorescence signal will be more efficient in eutrophic waters for monitoring chlorophyll-a concentration, however, because (a) chlorophyll-a has a dominant spectral signature, (b) simple atmospheric correction is not required, and (c) fluorescence increases with intensifying chlorophyll-a concentration [64].

Hyperspectral remote sensing is more reliable for monitoring chlorophyll-a concentration than multispectral remote sensing because it can measuring the reflectance of the extremely narrow wavebands[61], and therefore has high potential to monitor chlorophyll-a concentration in water bodies [63].

Suspended sediments play an important role in transporting nutrients and contaminants because a considerable amount derives from soil and bedrock erosion. The presence of suspended sediments in surface waters has negative effects on aquatic life. In addition, a high concentration of suspended sediments shortens the beneficial and efficient life of lakes and reservoirs [65]

Turbidity and SSSC are related to the suspended sediment fluxes in rivers lakes, and reservoirs, and can help monitoring the sediment discharge, and more generally the sediment budget within catchments, seasonal variability and evolution over time. In turn, the sediment budget is controlling the silting of the dams, which impacts the sustainability of hydroelectric structures and the supply of water for treatment plants. SSSC in inland waters also contributes to pollution and public health issues. Indeed, a signifi- cant correlation exists between the concentration of parasites and bacteria and several water quality parameters including SSSC and turbidity[66].

Suspended particles can carry viruses and bacteria pathogenic to humans [67] and foster their development [68].

High SSSC and turbidity can therefore be considered as a vector of microbiological contaminants which cause diarrheal diseases[65].

Water turbidity and SCCC in lakes or reservoirs may evolve through time, for instance in response to land use changes, modifi- cation of soil erosion, transport and deposition over the watershed, as well as exceptional rainfall events [65].

The quality ofin-situ monitoring networks depends on the number of sampling stations, their spatial representativeness and the frequency of the measurements. In many regions of the world, monitoring networks are decreasing[69], and in some regions, such as West Africa, they are very poor or non-existent.

The Surface Suspended Sediments (SSS) absorb and scatter light, thereby affecting the spectral response of surface waters. Turbidity refers to optical properties of water and has been shown to impact water reflectance in the visible and near-infrared domain. In that context, remote sensing may be a solution in mitigating the data gaps or lack of in-situ network in many areas worldwide[65].

Satellite data and field data were integrated for monitoring tributaries of the Amazon River in Peru, and found that MODIS images could be used to study the SSSC and, combined to river discharge data, to assess the sediment discharge[65].

The objectives of our study are Estimate turbidity, TSS and chlorophyll and analysis of its spatio-temporal variability in two reservoirs (Tucurui and Cefni) using LandSat satellite data. So we can do comparisons between the results obtained from two reservoirs and improve the already existing techniques, thus contributing to the state of the art.

Chapter 3

Materials and Methods

3.1 Study Area

Studies for the construction of a hydroelectric power plant on the Tocantins River to make use of the area's exploitation potential began in 1957, with the Tucuruí hydroelectric power plant inaugurated in 1984. This plant was built to supply energy for aluminum production, stimulate the regional industry, articulate the links and produce energy to power the country on a national scale [70]. The first stage of deployment occurred between 1975 and 1989, with twelve main units with a total capacity of 3960 MW. Subsequently, two auxiliary units increased capacity to 4000 MW. The second stage opened in late 2008 increased the installed capacity to 7960 MW. The damming led to the formation of a large lake of about 200 km in extension and an area of approximately 2875 km2.

The construction of the Tucuruí hydroelectric power plant caused a large increase in the surrounding population and displacement of the rural population due to flooding of the area, development of mining projects in adjacent regions and agricultural colonization in the vicinity of the Trans-Amazon Highway. The wide availability of fishing resources generated by the reservoir also attracted a large number of people looking for work, employment and income, causing extreme anthropogenic impacts in this area[70].

For development of this project were chosen two reservoirs: the reservoir of the hydroelectric plant of Tucurui[71], [72], viewed as a deep reservoir with a maximum depth of 77 m average depth of 198m and Cefni reservoir, viewed as a shallow reservoir [73].

3.1.1 The Tucurui reservoir

The Tucuruí hydroelectric power plant is located in the state of Pará, Brazil. The reservoir is located at coordinates: latitude 03^o 45' 03"S, longitude 49^o 40' 03"W. The plant was constructed in Tocantins river, about 7 km from the town of Tucuruí and 300 km from the city of Belem, the state capital. The reservoir has a total flooded area of approximately 2,850 m2, with approximately 50.8 million m3 of water. It is the first large-scale (25 units) hydroelectric project in the Brazilian Amazon rainforest, with an installed capacity of 8370 MW. The main purpose of the dam is hydroelectric power production to the Brazilian states of Maranhão and Pará and navigation between the upper and lower Tocantins river[71].

Tucurui is considered as a deep reservoir, with a maximum depth of 77 m and an average depth of 19-8 m. The power plant reservoir was built in Tocantins river, about 7 km from the city of Tucuruí. The reservoir has a total flooded area of approximately $2850km^2$, with approximately 50.8 million m^3 of water.

In the Brazilian amazon region there are 5 reservoirs in operation: Couracy Nunes, Curua Una, Tucurui, Balbina, and Samuel. The UHE Tucuruí plant is a large-scale hydroelectric power plant that is located in the state of Para on the Tocantins River[74].

3.1.2 Physico-chemical Parametres analyzed in Tucurui Reservoir

One of the main impacts in the Brazilian Amazon in the last decades has been the construction of hydroelectric power plants, with their accompanying dams and reservoirs, resulting in dramatic alterations to these ecosystems, such as loss of diversity and large-scale deforestation. Monitoring is fundamental for reservoir management and the evaluation of anthropogenic environmental impacts. The water quality of reservoirs in the Brazilian Amazon is greatly influenced by hydrological cycles, that in turn cause variations of microbiological, physico-chemical characteristics. There are, however, scarce reports in areas that suffer well-defined hydrological cycles, such as the Brazilian Amazon. In this context, this study presents an alternative method for predicting PTotal, FeTotal, Turbidity, Transparency, Fe2, Total Suspended Solids, PO4, Fe3, Temperature and Chorophylla in the Tucuruí Hydroelectric Power Plant reservoir, in the Brazilian Amazon, by applying Wavelet transformation of data obtained from remote sensing images, taking into account the hydrological cycles of the area, from 2007 to 2014, which were then analyzed by Artificial Neural Networks and compared to laboratory results.

The Figure 3.1, the components PTotal, FeTotal, Turbidity, Transparency, Fe2, Total Suspended Solids, PO4, Fe3 are strongly related to Factor 1. The analysis has been done using the IBM SPSS Statistics Software. This table contains the unrotated factor loadings, which are the correlations between the variable and the factor. Because these are correlations, possible values range from -1 to +1.

The figure 3.1 shows the loadings (extracted values of each item under 6 variables) of the 20 variables on the six factors extracted. The higher the absolute value of the loading, the more the factor contributes to the variable (We have extracted six variables where in the 20 items are divided into 6 variables according to most important items which similar responses in component 1 and simultaneously in components 2, 3, 4, 5 and 6).

The resuls obtained by Component Matrix showed good correlation for PTotal, FeTotal, Turbidity, Transparency, Fe2, Total Suspended Solids, PO4, Fe3, Temperature and Chorophylla, indicating that the proposed techniques can be used to analyze these components.

	Component					
	1	2	3	4	5	6
PTOTAL	.893	.086	-.019	-.025	-.130	-.095
FeTotal	.869	.081	-.020	-.038	-.102	-.088
Turbidity	.812	-.279	-.083	.043	-.035	.031
Transparency	-.799	.033	-.038	-.014	-.278	.263
Fe2	.763	-.095	-.202	-.055	-.202	.189
Total Suspended Solids	.760	-.136	.176	.036	-.006	-.242
PO4	.733	.011	-.147	-.155	.035	-.155
Fe3	.711	.119	.001	-.086	-.070	-.116
Temperature	-.533	.374	.291	-.011	-.044	-.483
K	.378	.675	-.112	.127	-.184	.141
Na	.165	.630	-.206	.430	-.053	-.140
Cloro	.055	.521	-.445	.371	.058	.360
pH	.361	-.516	.012	.070	.413	.418
Mg	.165	.235	.693	.133	.157	.114
NH4	.322	.117	.664	.198	-.032	.309
Ca	-.174	-.471	-.061	.571	.081	-.079
Dissolved Oxygen	.090	-.463	-.156	.463	.255	-.303
Chlorophyll	.092	.445	.047	.319	.626	-.071
Conductivity	.258	.284	.045	-.510	.528	.052
NO3	.304	-.143	.364	.337	-.401	.041

Figure 3.1. Component Matrix

3.1.3 Identification and Location of Collection Stations - Tucuruí

For this study, the following sampling stations were chosen: C1, C2, M1, M3, MR, MBB, ML, MBL, MP, MJV 3.2.

The water collections occurred at the ten points indicated above[75]. these water collection points have established important differences in morphometry of the system, which directly influenced the circulation of the flow of water in the region. The table 3.3 shows some of the relevant descriptions of each point, which will make it possible to understand of the results found:

3.1.4 Sampling Stations: Tucurui reservoir

Description of the collection stations in Tucurui Reservoir:

Sampling Station: Montante 1(M1)

Located 2 km upstream from the dam on the original Tocantins river channel. This is important in the monitoring, because it represents the water to be captured by the generating units and also the water to be sent downstream. When the reservoir is at the maximum operating level (74m in relation to the sea) depths up to 70m can be verified.

Sampling Stations: Caraipé 1 (C1) e Caraipé 2 (C2)

Table 3.1. Geographical location of sampling points located upstream and downstream of the Tucuruí Hydroelectric Power Plant dam, Brazil- Tucuruí

Sampling Stations	Name	Latitude	Longitude
C1	Caraipé 1	04°32.91’9”S	49°26.44’2”W
C2	Caraipé 2	04°29.46’2”S	49°31.54’2”W
M1	Montante 1	03°45.84’5”S	49°39.54’4”W
M3	Montante 3	04°25’21.7" S	49°30’29.4"W
MR	Montantante Novo Repartimento	04°13.05’7”S	49°41.96’3”W
MBB	Montante Breu Branco	03°49.75’0”S	49°38.89’5”W
ML	Montante Lontra	04°29’20.2"S	49°31’17.5"W
MBL	Montante Belauto	04°14’04.3"S	49°27’55.0"W
MP	Montante Pucuruí	04°21’22.8"S	49°46’05.7"W
MJV	Montante Jacundá Velho	04°32’58.5"S	49°26’24.5"W

Table 3.2. Water collection stations along the reservoir of the Tucurui Hydroelectric Power Plant - BRAZIL - PA

MSE Validation by Cycle					
Parameters	Sampling Stations	Full	Emptying	Dry	Filling
CHLOROPHYLLa	C1	1.1593	17.1529	0.2679	5.4940
	C2	0.1555	4.3905	0.4366	0.0889
	MBB	0.3346	0.0070	0.8778	0.1564
TRANSPARENCY	MJV	0.1789	0.0736	0.0156	0.0828
	M1	0.0010	0.4436	0.4957	0.0272
	M3	0.0966	0.2470	0.2272	0.2318
TSS	M3	0.0444	1.1343	0.0006	1.6069
	MJV	0.0106	1.1881	0.0471	0.2483
	MIP	1.1363	0.0135	11.3284	0.7024

Located on the left bank of the reservoir in the region currently called "Caraipé Region" where since 2002 the Sustainable Development Reserve (RDS) . In this region there are many inhabitants, around 5.000 inhabitants, with a high level of anthropization characterized by the high level of deforestation in this region. The two stations are located in the old channel of the Caraipé region presenting depths of up to 28m and 22m (when the reservoir is full).

Sampling Stations: Montante Breu Branco (MBB)

Located on the right bank of the reservoir, in front of the city of Breu Branco, region where much of the surface drainage of the city is launched. The sampling station has a maximum depth of 32 m. This region is located near the urban nucleus of the municipality of Breu Branco, with few areas of primary forest.

Sampling Stations: Montante Belauto (MBL)

Located on the right bank of the reservoir, full protection area (ie, no residents allowed). In this region, there are large areas with primary forest, however this part of the reservoir is characterized by having a retention time superior to the average of the reservoir, contributing to the fact that the water in this region presents different physico-chemical characteristics. It has a maximum depth of 26 meters.

Table 3.3. Characteristics of the sampling points of the Hydroelectric Tucuruí - Pará - Brazil

Sampling Stations	Name	Characteristics
C1	Caraipé 1	Islands
C2	Caraipé 2	Islands
M1	Montante 1	Next to dam
M3	Montante 3	Lake - Central channel
MR	Montantante Novo Repartimento	Lake - left bank of the reservoir
MBB	Montante Breu Branco	Next to dam
ML	Montante Lontra	Lake - Central channel
MBL	Montante Belauto	Lake - right bank of the reservoir
MP	Montante Pucuruí	Lake - left bank of the reservoir
MJV	Montante Jacundá Velho	Lake

Sampling Stations: Montante Repartimento (MR) e Montante Pucuruí (MP)

Located on the left bank of the reservoir, in the region of the Sustainable Development Reserve (RDS). This region is the most dendritic of the reservoir, that is, it occupied large area, but presents low depth. However, the two stations have maximum depths of 20m (MP) and 32m (MR) due to their location in the old pipeline of the Pucuruí and Pucuruizinho streams, respectively. In this region, there is a place of fish landing "in natura" called "Polo Pesqueiro" to follow the municipality of Novo Repartimento.

Sampling Stations: Montante Jacundá Velho (MJV)

Located on the right bank, where there was the old urban nucleus of the city of Jacundá. In this region, there are two landing sites for fresh fish, one of which is called "Porto Novo" and "Porto da Colônia". This region is quite anthropized with small areas of native vegetation. The sampling station is located in the old Jacundá river channel with a depth of up to 22 m (when the reservoir is full).

Sampling Stations: Montante Lontra (ML)

Located on the right bank, near the Indigenous Land of the Parakanã Indians (today the largest extension continues with native vegetation in the Lake of Tucuruí region), located in the old Bacuri channel, presenting a maximum depth of 22 m (when the reservoir is full).

Sampling Stations: Montante 3 (M3)

Located in the central part of the reservoir, distant approximately 60 km straight from the Tucurui dam, located in the old Tocantins river, it has a maximum depth of up to 52 meters (when the reservoir is full).

Sampling Stations: Montante Ipixuna (MIP)

Located in the central part of the reservoir, approximately 130 km straight from the Tucurui dam, located in the old trough of the river Tocantins. When in the filling period of the reservoir, it presents depths of up to 42 meters. This presents the characteristic of behaving like reservoir in the period of full and like river in the dry period.

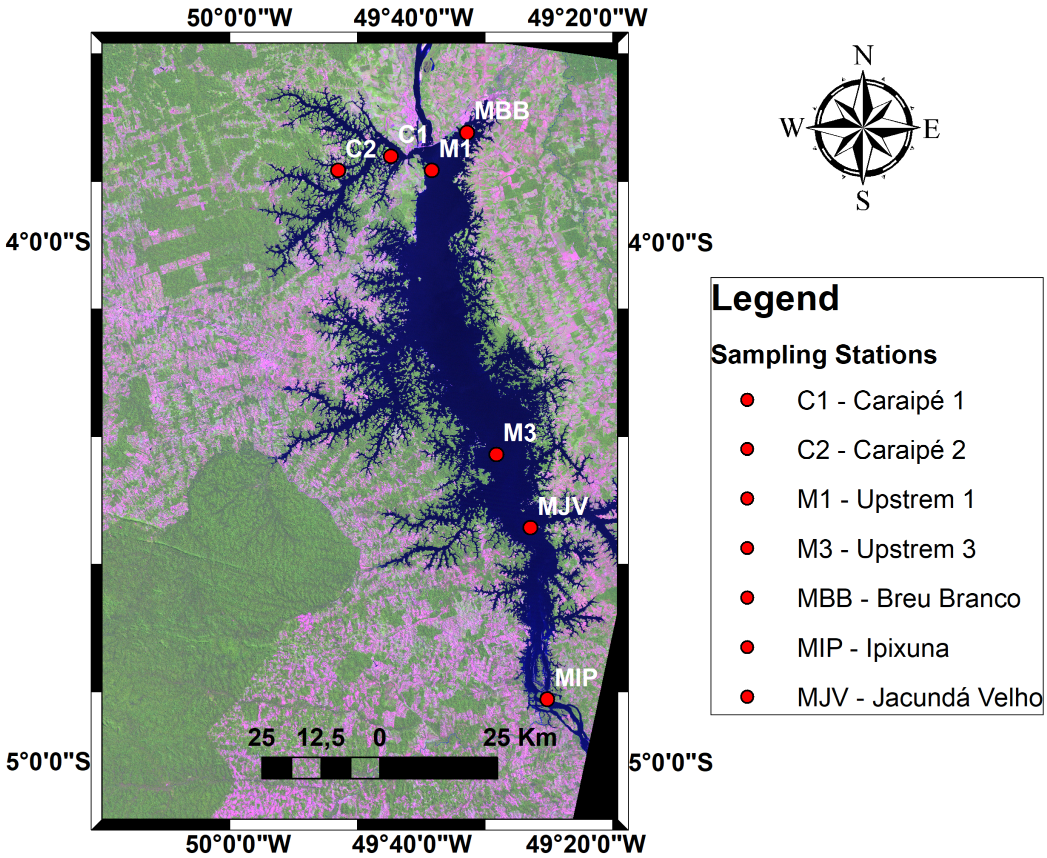

Figure 3.2. Sampling Stations Tucurui Reservoir - Amazon Region

3.1.5 Pre-processing satellite images: Tucurui Reservoir

The satellite images were obtained from the ESPA (https://espa.cr.usgs.gov), captured by the LandSat 7 of the reservoir from 2007 to 2014. Four images were collected per year, corresponding to each hydrological cycle for all sampling stations.

Initially a point is chosen for analysis, from this it is cut out an image A in its surroundings corresponding to 32x32 pixels. Obtaining an array containing 1024 pixels of information. For the next step, the wavelet transform with 1 level of decomposition is applied, resulting in a reduced image of 16x16 pixels, with 3 images (H, V, D) of 16x16 pixels representing the Horizontal, Vertical of reduced image.

For the input of the neural network, the matrices H, V and D were converted to their respective column-arrays and then merged with H, V and D images, generating a T column vector of size 768. This procedure was performed for the images of 2007,2008,2009, 2010, 2011, 2012, 2013, 2014, generating an input M matrix.

During the validation of the Neural Network, the images of 2014 were used, and it is necessary to perform the same image processing performed on the previous images. The process described from image A to generation of the M matrix and subsequent submission to the analysis and training in the neural network was performed by hydrological cycle for each point of water collection.

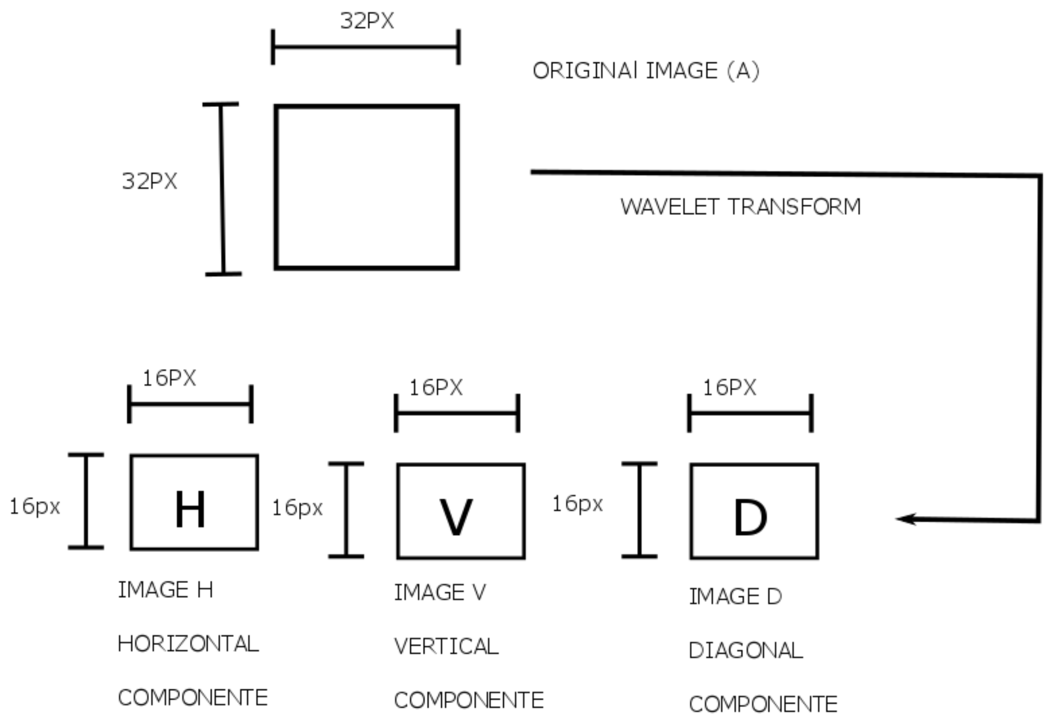

Figure 3.3. Pre processing: Satellite Image

3.1.6 Wavelet transform and ANN applied to the remote sensing images

The wavelet transform is an integral transform whose kernel is a class of special functions, called wavelets [76]. The main advantage of this method compared to other methods is its spectral location capability in space and frequency, which allows for the analysis of non-stationary signals in their various scales [77]. The wavelet transform used in the present study was the discrete transformed, with allows for the multi-resolution analysis of a signal, decomposing said signal into approximations and details. The approximations are high ranges, i.e., low-frequency signal components. The details are the low ranges, i.e., high frequency components[78]. The Haar family with a degree of decomposition in the Matlab software package was used [79].

One sampling station was initially chosen for analysis and a geographics image of the water sampling station, of 32x32 pixels, was cropped, corresponding to an array containing 1024 pixels. Each digital pixel value corresponds to an average of radiance values, emittance or backscatter of the different targets that can be contained in the pixel from the vicinity of the water sampling stations, as displayed in an example in Fig. 3.6

Subsequently, the wavelet transform was applied, with only one level of decomposition, resulting in a matrix array of 16x16 pixels for each of the following three components: Horizontal (H), vertical (V) and diagonal (D).

The conversion of the arrays to the H, V and D components to their respective column-matrices was performed, and subsequently a concatenation of the three arrays (each containing 256 pixels) was executed, generating a vector with column

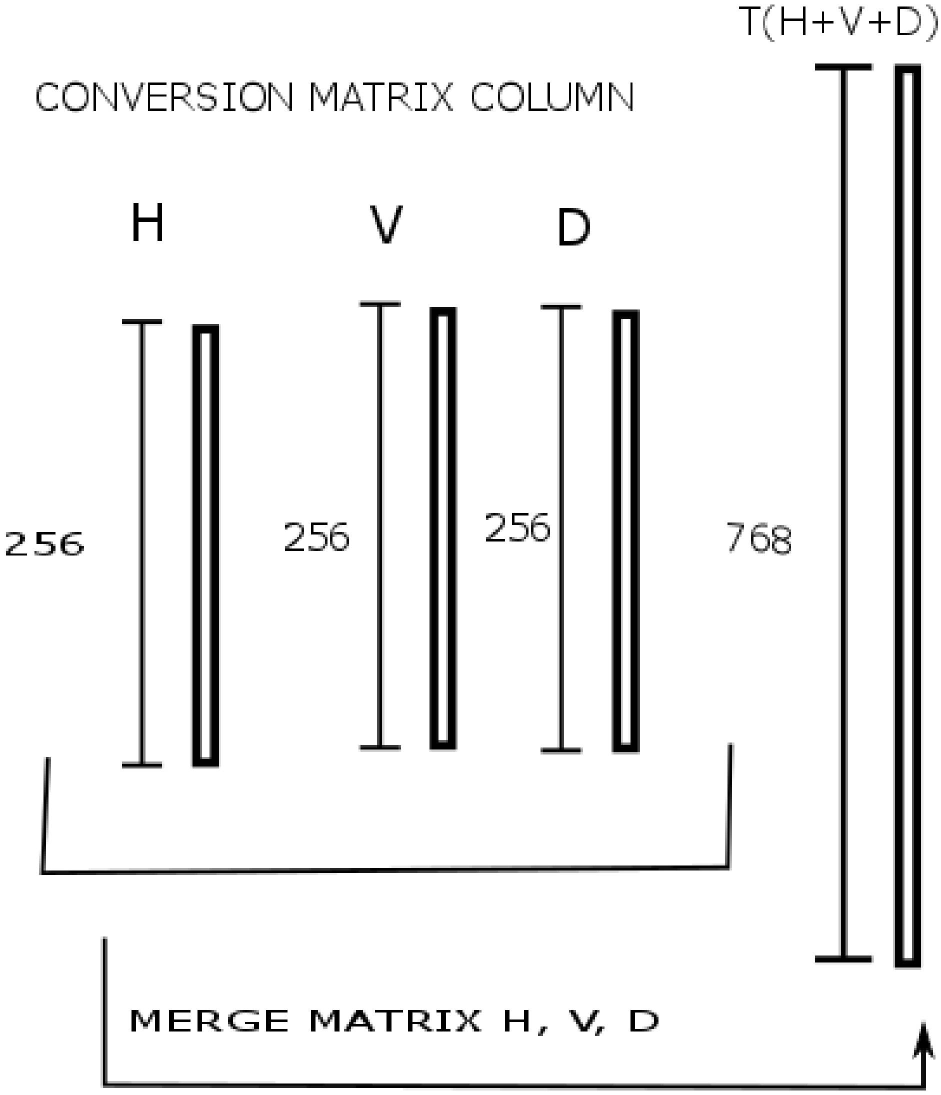

Figure 3.4. Pre Processing Satellite Image: Conversion Matrix Column

size (256 x 3).

This data, the image of the geographical area containing the water sampling collection point, decomposed via wavelet into its three wavelet components, was used as the ANN input. Tests were conducted considering the image representations isolated for each wavelet component, with satisfactory results.

However, when the input data of the three wavelet components was considered, the approximations were even better, which motivated the choice of this arrangement in the proposed solution.

The digital values of the pixels of the images cut in the vicinity of the collection stations of water samples were used as input for the ANN. The digital pixel value is an average of radiance values, emittance or backscatter of the different targets

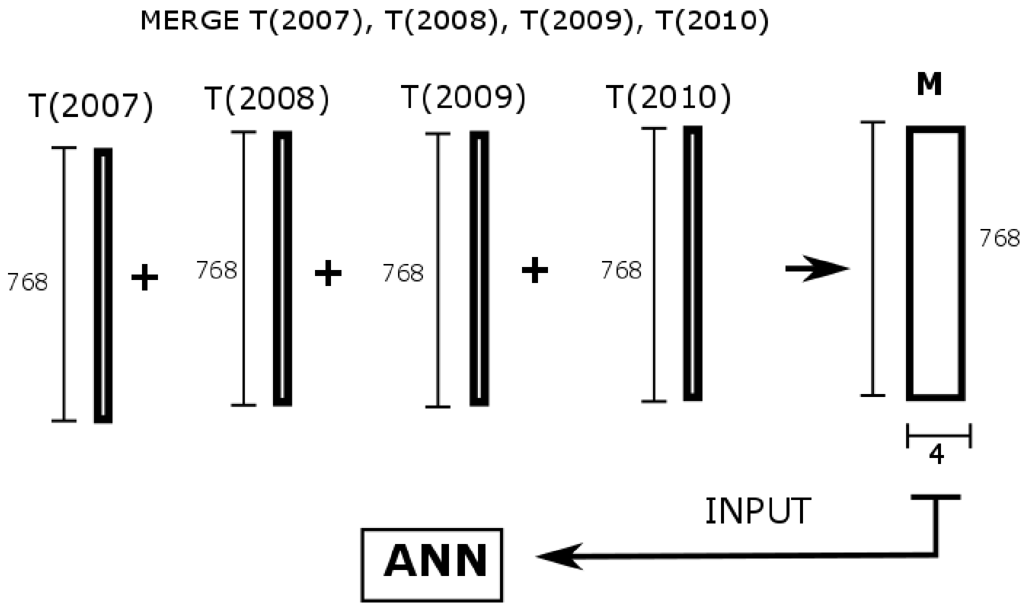

Figure 3.5. Pre processing3: Satellite Image

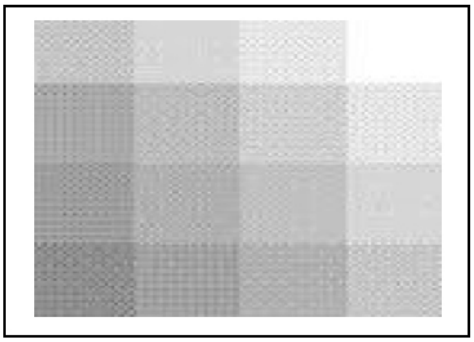

124	135	141	255
110	120	128	141
109	115	120	135
98	110	119	128

Figure 3.6. Example of a pixel matrix and it corresponding digital values

that can be contained in the pixel. Thus, the possible differences between the digital values of the images of the different hydrological cycles used in the study were related to the output data of chlorophyll-a levels, water transparency and total suspended solids, forming the input/output pairs for the ANN training. The figure 3.7 displays a pixel matrix and its corresponding digital values.

The data obtained in the laboratory (estimated) refer to the ANN execution, which are then compared to the data really observed in 2014. This validates the ANN output data.

The images from the satellites were obtained during the same timeframe as the water samplings. For example, if a water sampling was conducted in March 2008, a satellite image was retrieved in March 2008.

After processing, satellite images were used as inputs to the neural network.

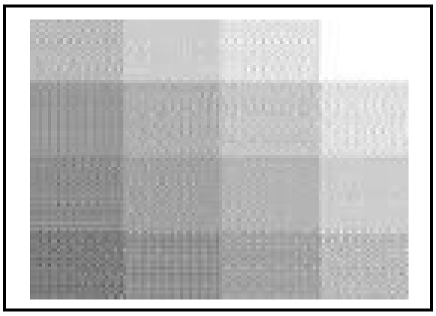

124	135	141	255
110	120	128	141
109	115	120	135
98	110	119	128

Figure 3.7. Digital values of the pixels of the images cut in the vicinity

3.1.7 Neural networks

Neural networks are parallel distributed systems consisting of two basic types of components: the processing units, arranged in one or more layers, interconnected, called neurons; and the synapses, which are the connections between the processing units. In the present study, the ANN paradigm applied was the Direct Multilayer Perceptron, developed using the Matlab software package (Matworks, 2009). Post-processed images of the ten sampling sites per water cycle were used for the ANN input and the output variables were the variables chlorophyll-a, total suspended solids and transparency. The architecture of the ANN consisted of three layers: the input layer, the hidden layer and the output layer. The validation process of the ANN was conducted with 2014 images processed according to the method described in section 2.4. Figure 3.8 displays the architecture ANN with the column vector Pi (i = 1,2, .., 728) as input. The ANN was trained with the following parameters:

- Learning rate: 0.01.
- Transference function: tansig in all the neurons of the hidden layer and purelin in the output layer.
- Network training function: Gradient descent with momentum and adaptive learning rate backpropagation.

The digital values of the pixels of the images cut in the vicinity of the collection stations of water samples were used as input data for the ANN. Thus, the possible differences between the digital values of the images of the different hydrological

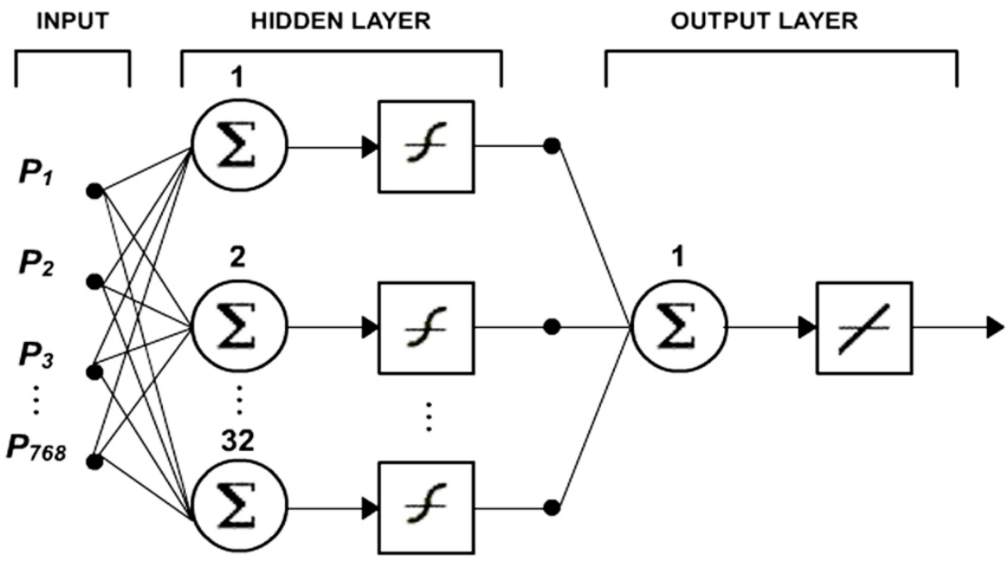

Figure 3.8. Schematic of the ANN architecture used in the present study

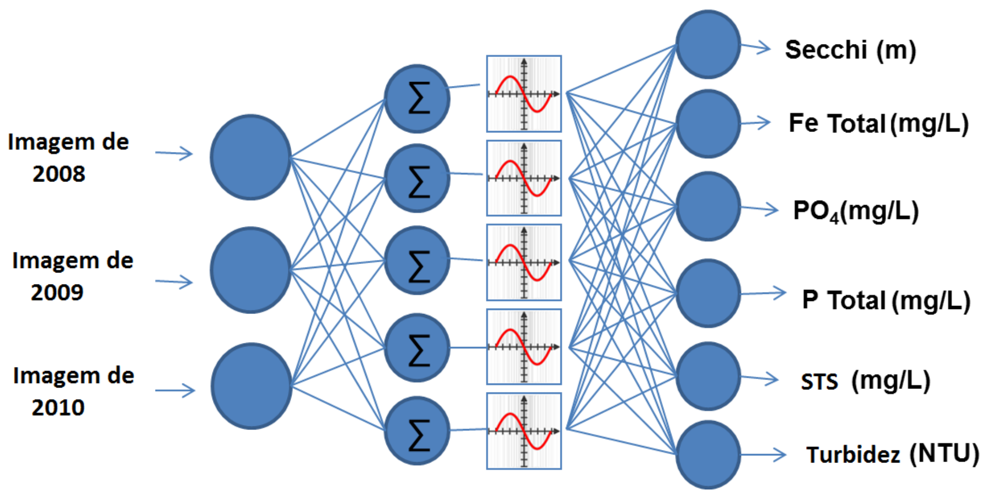

Figure 3.9. Schematic of the ANN architecture used in the present study

cycles used in the study were related to the output data of chlorophyll-a levels, water transparency and total suspended solids, forming the input/output pairs for the ANN training.

The Figure 3.10 shows the procedure performed with the 2007, 2008, 2009, 2010, 2011, 2012, 2013 images, generating an ANN input matrix with 768x7 dimensions for each measurement of the hydrological cycle (full, emptying, dry and filling) of the investigated study years. Water samples were collected from the 12 sampling points, but for 2 points located south of the reservoir (downstream) there were missing images within the four analyzed years, which would undermine the analysis in the study. So only the following points sampling points were analyzed:C1, C2,

M1, MBB, MR, MP, M3, ML, MJV , MIP.

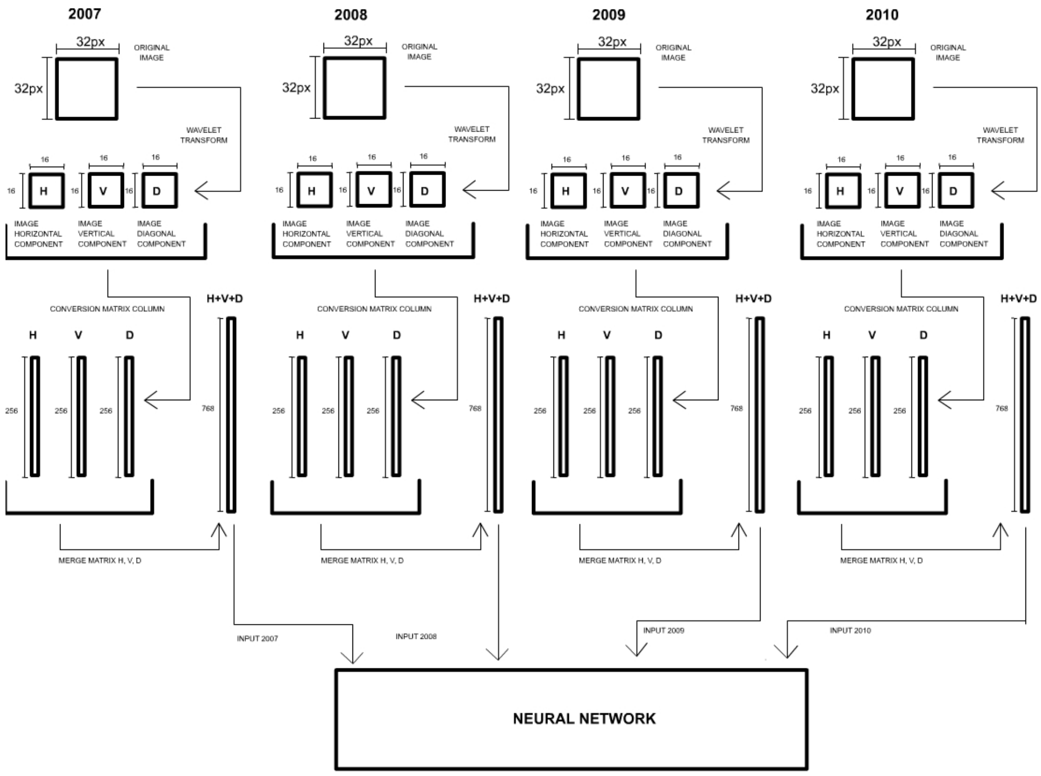

Figure 3.10. Conversion of the image of a water sampling station, by integrating the wavelet transform and artificial neural network techniques

3.2 The Cefni reservoir

Cefni Reservoir is a reservoir in the centre of Anglesey, Wales which is managed by Welsh Water and Hamdden Ltd, while the fishery is managed by the Cefni Angling Association, area: 86 ha and length: 2.3 km Cefni Reservoir on the Isle of Anglesey was overflown as part of the UK Natural Environment Research Council (NERC). The lake is shallow, with a maximum depth of approximately 4 m and contains beds of submersed, floating-leaved and emergent aquatic macrophyte species. It is also known to support dense growths of toxic blue-green algae during summer. The reservoir is surrounded by an approximately 100-m wide plantation of coniferous trees with agricultural fields beyond[73].

3.2.1 Physico-chemical Parametres

Physico-chemical parameters of the water such as PH , CONDUCTIVITY, COLOUR, CHLOROPHYLLA are important variables for the analysis of Freshwater ecosystems, that are significant not only for human populations but also essential for plant and animal diversity.

Figure 3.11. Conversion of the image of a water sampling station, by integrating the wavelet transform and artificial neural network techniques

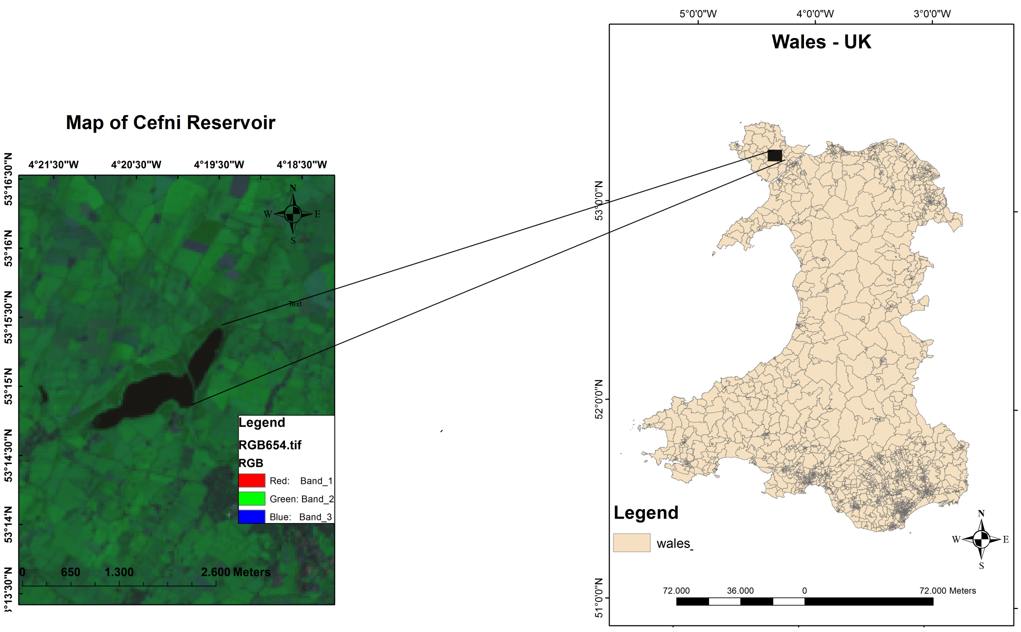

Figure 3.12. Conversion of the image of a water sampling station, by integrating the wavelet transform and artificial neural network techniques

Freshwater lakes are significant not only for human populations but also essential for plant and animal diversity. These aquatic systems are unique and rich in biodiversity at the same time are under constant threat due to bludgeoning human populations and their demand for land[80].

The concentration of the hydrogen ion in water is usually measured in terms of pH. The pH or negative logarithm of the hydrogen ion concentration is a master variable in water quality because the hydrogen ion influences many reactions. The optimum pH range for most aquatic organisms is 6.5–8.5, and the acid and alkaline death points are around pH 4 and pH 11, respectively. Most living organisms do not tolerate large variations in pH and may die. [81][82].

The pH of natural waters is strongly influenced by the concentration of carbon dioxide, which is considered an acid gas[82]. Because dissolved carbon dioxide is acidic, rainwater that is saturated with this gas is naturally acidic—usually about pH 5.6.[81].

Water bodies with moderate to high alkalinity are well-buffered against wide daily swings in pH resulting from net removal of carbon dioxide by photosynthesis during daytime and return of carbon dioxide to the water by respiratory process at night when there is no photosynthesis. [81]

Conductivity defines the ability of water to conduct electricity.This parameter provides a good indication of changes in the composition of water as pollutant particles. This type of measurement accesses the concentration of ions in a solution. More the ions higher will be the conductivity. For water to be pure it's conductivity should be poor.

Generally there are two types of conductivity sensors: two electrodes and multiple electrodes from which two electrodes sensor is commonly used. It is made by using two platinum plates deposited on two parallel glass or inner wall of glass tube. Conductivity of water measures in μs/cm or mA [83].

Colour is water quality parameters that detract from the appearance of water, colour refers to Transparency condition of water,organic material that has dissolved into solution and important in determining Secchi disk depths among reservoir [84].

The Chlorophyll-a (Chl-a) concentration is commonly used as a proxy for phytoplankton biomass and as indicator for eutrophication and it can be retrieved from remote sensing data[85].Chl-a is a direct indicator used to evaluate the ecological state of a waterbody, such as algal blooms that degrade the water quality in lakes, reservoirs and estuaries[86].

Many scientists have studied on the influence of freshwater physico-chemical parameters to the changing ecosystems. Studies involving the statistical analysis, wavelet signals, neural network, remote sensing and water sampling have been used in the monitoring of ecosystems [25][26][27][28] [29].

Several operational monitoring systems based on remote sensing are in place to monitor the reservoir. However, evaluations of reservoir monitoring systems based on satellite data are scarce. The methods currently used for water analysis are time-consuming, extremely costly, because it requires sample collection, trained people and specialized laboratories. Predicting these parameters helps decision-making in the present and planning in the future.

Artificial neural network algorithm can be used for simulates human learning processes through establishment and reinforcement of linkages between the input and output data and can make relationship of a dependent variable with independent variables.

Even with a correct model applied by a well-trained analyst, all predictions remain subject to fundamental uncertainties, especially with regards to variation in aspects such as actual weather conditions[87].In order to reduce this uncertainty, many investigations are conducted to find a more efficient model that allows the researchers to infer with greater precision the estimation of water quality parameters.

Predictions based on time series are efficient for treatment of uncertainty. Thus arises interest in prediction physico-chemical parameters, in which the difficulty involves to estimate these parameters through the reflectance of satellite images associating a set of data available in data collection.

In the context of water quality parameters, we propose an alternative for retrieval through prediction with ANFIS that are adjusted, or trained, so that a given input leads to a specific target output.

To this end, a case study with the data of the Cefni reservoir was applied, aiming to clarify the benefits of the ANFIS, emphasizing its efficiency and simplicity of implementation.

3.2.2 Pre-processing satellite images: Cefni Reservoir

For Cefni Reservoir we intent analyze remote sensing images were obtained from the ESPA satellite image bank, captured by a Landsat 8 satellite and Sentinel 2 satellite from 2007 to 2016, using the spectral band 1, band 2, band 3 and band 4. The combination of the three basic colors (blue, green and red), landsat 8, for Cefni reservoir is shown in figure 3.13

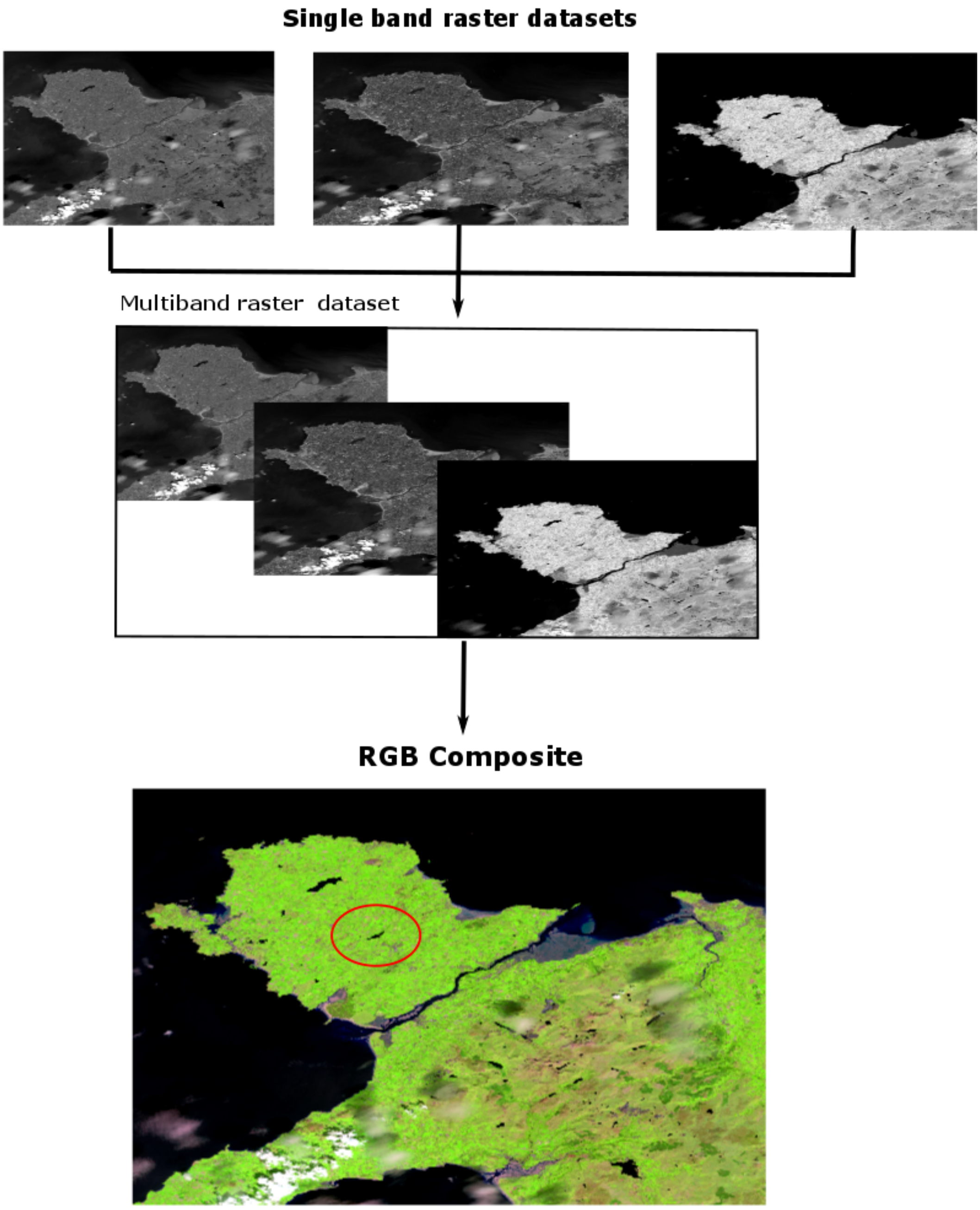

Figure 3.13. Cefni Reservoir: Pre processing satellite imagens

Chapter 4

Application of the Methodology and Results

4.1 Factor Analysis

Descriptive statistics were used to analyze the physico-chemical Parameters of water. Factor analysis on the database for validity was performed using tests contained in SPSS. Exploratory Factor Analysis (EFA) was applied to the all parameters. Tests Used In Factorial Analysis: Bartlett's sphericity test and Kaiser-Meyer-Olkin (KMO). Kaiser-Meyer-Olkin (KMO): This measure is represented by an index (KMO) that assesses the adequacy of the factorial analysis, being calculated by:

$$KMO = \frac{\sum\sum_{j\neq k} r_{jk}^2}{\sum\sum_{j\neq k} r_{jk}^2 + \sum\sum_{j\neq k} q_{jk}^2} \tag{4.1}$$

where the correlation matrix is $R = [r_{ij}]$ and the partial covariance matrix is $Q = [q_{ij}]$. The overall KMO measure of sample adequacy is given by the above formula taken over all combinations and $j \neq\ k$.

If the partial correlation is near to zero, the PCA can perform efficiently the factorization because the variables are highly related: $KMO \cong 1$.

First, the Keiser-Meyer-Olkin (KMO) test for sampling adequacy and Bartlett's test for sphericity was done. The KMO value was 0.78, in this case, KMO is over then 0.5, indicate that Factor Analyses Method is appropriate for this analyses.

The Bartlett's test checks if the observed correlation matrix R=(rij)(p x p) diverges significantly from the identity matrix (theoretical matrix under H0: the variables are orthogonal). Principal Component Analysis (PCA) is the most widely used unsupervised dimensionality reduction approach. In recent research, several robust PCA algorithms were presented to enhance the robustness of PCA model[88]. The PCA can perform a compression of the available information only if we reject the null hypothesis [89].

In order to measure the overall relation between the variables, we compute the determinant of the correlation matrix |R|. Under H0, |R| = 1; if the variables are highly correlated, we have |R|= 0. The Bartlett's test statistic indicates to what extent we deviate from the reference situation |R| = 1. It uses the following formula.

$$X^2 = -\left[(n-1) - \left(\frac{2P+5}{6}\right)\right] \ln |R| \quad (4.2)$$

Where:
n: sample size
p: number of variables
|R|: determinant of the correlation matrix

Under H0, it follows a distribution with a [p x (p-1) / 2] degree of freedom.

The Bartlett test presented significant value. Six factors were obtained with total variance explained of 68.68. Fig. 4.2 shows the factors, total and cumulative variances. The method of factor extraction was Principal Components and the orthogonal varimax rotation.

In Fig. 4.4 Component Matrix, the parameters PTotal, FeTotal, Turbidity, Transparency, Fe2, Total Suspended Solids, PO4 and Fe3 accounted for the greatest amount of common variance compared to the rest of components.

This is again reflected in Fig. 4.3 the scree plot for physico-chemical Parameters. It had six values above the eigenvalue of 1. Even though the seven score (0.92), and eight score (0.86) and nine score (0.71) were below eigenvalue of 1 and did not contribute sufficiently to the model, its presence, nevertheless, was indicative that with sufficient power, its score could increase to above eigenvalue of 1. This could result in the formation of more three components.

The Principal Component Analysis(PCA) extraction method component matrix clearly demonstrated that PTotal, FeTotal, Turbidity, Transparency, Fe2, Total Suspended Solids, PO4, Fe2 and Fe3 parameters were related to Factor 1, observed in Fig. 4.5 , this means a strong correlation between these parameters.

The figure 4.1 refers to commonalities, which are quantities of variance, that is, correlations of each variable explained by the factors. High value of commonality means that the variable has great power of explanation. The minimum acceptable value is 0.5 and the maximum is 0.8.

The figure 4.4 in this case showed the relation of the elements PTotal, FeTotal, Turbidity, Transparency, Fe2, Total Suspended Solids, PO4 and Fe3, grouped in Factor 1 (F1), with a strong correlation between these parameters. We can conclude that these elements present great reflectance in bodies of water, being possible the analysis through satellite images.

Table 4.1. KMO and Bartlett's Test

KMO and Bartlett's Test		
Kaiser-Meyer-Olkin Measure of Sampling Adequacy.	0.78	
Bartlett's Test of Sphericity	Approx. Chi-Square	1414.6
	df	190.00
	Sig.	0.00

Figure 4.1Extraction Method: Principal Component Analysis.

Figure 4.2 Extraction Method: Principal Component Analysis.

Figure 4.4Extraction Method: Principal Component Analysis. 6 components extracted.

Figure 4.5 Extraction Method: Principal Component Analysis. Rotation Method: Varimax with Kaiser Normalization. Rotation converged in 8 iterations.

Figure 4.6 Extraction Method: Principal Component Analysis. Rotation Method: Varimax with Kaiser Normalization.

Figure 4.7 Extraction Method: Principal Component Analysis. Rotation Method: Varimax with Kaiser Normalization. Component Scores.

4.2 Artificial Neural Network Results

The integration of water quality parameters is essential in environmental monitoring and very important for decision-making. Advanced techniques to manage are required in complex evaluation process. We here propose a ANN hybrid model to assess reservoir water quality using Remote Sensing and Wavelet Transform.

Surface water quality is a major environmental concern as it is a main source of fresh water for human consumption governed by the complex anthropogenic activities and natural processes[90].

The changes in the water body ecosystem especially in rivers and lakes have a major impact on human welfare and the aquatic environment [91]. Continuous deposition of solid waste material and contaminants in the water of lakes and rivers has become a global health concern as these are a major source of water supply for human consumption and domestic purposes [92].

In Brazil due to a large demand for electricity, there is a growing number of hydroelectric power plants in the water reservoirs to generate energy. Monitoring the reservoirs is important for the decision-making process.

The parameters selected for analysis are strongly related to the water quality monitoring, such Chlorophyll-a, TSS and transparency, PTotal, FeTotal, Turbidity, Transparency, Fe2, PO4, Fe3. For example Clorophyll-a levels are responsible for the photosynthetic process and reflect the phytoplankton biomass in the ecosystem, while water transparency allows for estimations regarding the depth of the photic zone, i.e. the vertical depth of sunlight penetration in the water column, which indicates the level of photosynthetic activity in the reservoir [93] and, TSS can, among other effects, cause damage to aquatic life by settling at the bottom of the reservoir, destroying organisms and retaining bacteria and organic waste by promoting anaerobic decomposition [93], [24]. In this sense, these characteristics are routinely used to measure the trophic status of lakes.

These parameters, as mentioned previously, require extensive fieldwork in collecting the samples, which are then analyzed by trained personnel in laboratory conditions. Usually, the applied measurement techniques for some of these parameters are sophisticated, such as determination of clorophyll-a by spectrophotometry after extraction with hot ethanol and turbidity by nephelometric method, then scattered angle from the beam directed at the water sample [94].

In this research we propose the use of remote sensing techniques for the monitoring and prediction of water quality parameters. Nowadays, with advanced hardware and software, processing and analyzing satellite images have become easier and less costly, alongside the improvement of spatial and temporal resolution of the satellite imagery, in addition to algorithm optimization, has led to the acknowledgment of the incredible potential of this technique to monitor and, consequently, improve, water quality [95].

Global estimations of chlorophyll concentrations for example, have been investigated by several marine-specific satellite missions for the visible wavelength range, including SeaWiFS, MERIS and the planned Ocean and Land Colour Imager [96], [97].

Trophic classifications have been obtained based on these methods, by applying IRS-1C satellite imaging in monitoring chlorophyll content, for example, in specific water bodies, such as lakes, while anthropogenic impacts have also been demonstrated using these techniques, such as in the very recent study conducted in the Amazon that analyzed 40 years of Landsat-MSS/TM/OLI images to monitor the impacts of mining activities near the Tapajós River and observed that TSS concentrations were directly related to the mining activities [98].

The coupling of remote sensing with other statistical and computation techniques has, increasingly, been applied and proven valid in monitoring water quality. The alternative method described in the present study with wavelet transformation of the remote sensing images and analysis by ANN, thus, would contribute positively to laboratory analysis in the determination of the mentioned parameters, which is obviously advantageous for numerous reasons. Thus, the application of predictive methods as the one proposed in the present study are of interest since they provide alternative methods to obtain good accuracy and are less expensive than the procedures presently used in environmental monitoring programs conducted in these ecosystems.

Accordingly, the proposal established herein is to work with past data from previous years, classified per hydrological cycle, to predict the values for future hydrological cycles, hence, the fact that we used data from previous hydrological cycles, from 2007 to 2014 in the Tucurui reservoir, and data from the 2014 hydrological cycle for validation. The ANN training results of the wavelet transformed remote sensing images for each sampling stations and the four stages of the well- defined hydrological cycle were considered adequate, with low mean square errors (MSE) displayed in Table 4.2 for the following sampling stations: C1, C2, M1, M3, MBB, MIP, ML, MP, MP in the Tucurui Reservoir - Amazon region.

Following ANN training, the methodology was validated by comparing laboratory-obtained results for chlorophyll-a levels, TSS and transparency with the results obtained by the proposed methodology for the year 2014. Table 4.3 displays the approximation errors between the values obtained in the laboratory and those calculated by the proposed methodology per sampling station and hydrological cycle for the year 2014. The approximation errors were calculated as follows 4.3 :

$$Err(i) = V\_lab(i) - Y(i) \tag{4.3}$$

Where:
V_lab (i): Is the value obtained in the laboratory for this parameter
Y(i): Is the output variable obtained by the ANN.

The figures 4.8, 4.9, 4.10, 4.11 shows the validation results for 2014 for Chlorophylla in the C1, C2, MBB, MR sampling stations, with the laboratory results

Table 4.2. Mean Square Errors (MSE) in the ANN training conducted in the present study

		MSE			
Parameters	Station	Full	Emptying	Dry	Filling
	Transparency	2.73×10^{-24}	2.34×10^{-23}	4.60×10^{-22}	4.65×10^{-23}
C1	TSS	1.29×10^{-24}	3.57×10^{-23}	3.72×10^{-22}	9.18×10^{-25}
	Chlorophylla	$3.49 \times^{1} 0-22$	4.31×10^{-23}	3.93×10^{-24}	2.4×10^{-23}
	Transparency	1.43×10^{-22}	3.51×10^{-21}	4.08×10^{-22}	1.58×10^{-21}
C2	TSS	1.88×10^{-23}	8.44×10^{-23}	1.68×10^{-23}	6.52×10^{-23}
	Chlorophylla	8.69×10^{-24}	5.24×10^{-24}	1.84×10^{-23}	2.25×10^{-23}
	Transparency	1.14×10^{-22}	9.09×10^{-23}	1.47×10^{-22}	1.90×10^{-22}
M1	TSS	9.89×10^{-23}	9.95×10^{-22}	2.57×10^{-21}	1.18×10^{-22}
	Chlorophylla	1.63×10^{-24}	9.49×10^{-23}	2.25×10^{-24}	4.74×10^{-24}
	Transparency	1.45×10^{-21}	1.21×10^{-23}	1.32×10^{-22}	6.02×10^{-23}
M3	TSS	2.32×10^{-24}	9.94×10^{-23}	2.14×10^{-23}	8.16×10^{-25}
	Chlorophylla	7.00×10^{-24}	3.44×10^{-23}	3.05×10^{-24}	2.71×10^{-22}
	Transparency	4.14×10^{-22}	5.59×10^{-22}	$1.20 \times 10-23$	5.00×10^{-23}
MBB	TSS	3.22×10^{-24}	9.94×10^{-24}	6.05×10^{-24}	2.55×10^{-22}
	Chlorophylla	2.92×10^{-25}	1.22×10^{-22}	1.33×10^{-23}	3.65×10^{-24}
	Transparency	2.41×10^{-21}	1.25×10^{-22}	1.77×10^{-22}	2.27×10^{-21}
MIP	TSS	5.97×10^{-25}	6.10×10^{-22}	6.74×10^{-23}	6.18×10^{-22}
	Chlorophylla	9.75×10^{-24}	8.09×10^{-23}	3.83×10^{-24}	4.03×10^{-24}
	Transparency	3.65×10^{-23}	3.36×10^{-21}	1.19×10^{-22}	1.99×10^{-22}
ML	TSS	1.27×10^{-22}	2.24×10^{-22}	2.15×10^{-22}	2.06×10^{-22}
	Chlorophylla	2.47×10^{-24}	5.43×10^{-24}	1.99×10^{-24}	1.48×10^{-24}
	Transparency	3.86×10^{-22}	2.51×10^{-22}	2.64×10^{-22}	3.08×10^{-22}
MP	TSS	3.02×10^{-24}	2.04×10^{-22}	8.44×10^{-25}	1.85×10^{-23}
	Chlorophylla	1.33×10^{-22}	7.57×10^{-24}	7.61×10^{-24}	4.28×10^{-24}
	Transparency	2.76×10^{-23}	2.34×10^{-24}	4.20×10^{-22}	4.09×10^{-21}
MR	TSS	1.35×10^{-22}	4.92×10^{-23}	3.99×10^{-23}	8.55×10^{-24}
	Chlorophylla	3.16×10^{-24}	8.84×10^{-24}	2.47×10^{-23}	2.10×10^{-22}

being the "observed values" and those obtained by wavelet transformation of the remote sensing images and subsequent analysis by ANN, proposed herein, being the "estimated values", regarding chlorophyll-a, total suspended solids and transparency. The X-axes of figures represent the hydrological cycles (1, 2, 3 and 4, respectively, the full, emptying, dry and filling stages). The Y-axis represents the quantitative value of the analyzed parameter in a given hydrological cycle.

The figures 4.12, 4.13, 4.14, 4.15, 4.16, 4.17 shows the validation results for 2014 for TSS in the M1, M3, MIP, MJV, ML, MP sampling stations.

The figures 4.12, 4.13, 4.14, 4.15, 4.16, 4.17 shows the validation results for 2014 for TSS in the M1, M3, MIP, MJV, ML, MP sampling stations.

The figures 4.18, 4.19, 4.20, 4.21, 4.22, 4.23 shows the validation results for 2014 for Transparency in the M1, M3, MBB, ML, MP, MR sampling stations.

As previously stated, we propose remote monitoring of the reservoir using LandSat7 to predict the physico-chemical parameters of the water in seven (7) points as can be seen in fig 3.2. The following sampling stations C1, C2, M1, M3, MBB, MJV, MIP were selected.

The collection of water in these points were done periodically 4 times a year corresponding to the hydrological cycle: full, empyting, dry and filling. The different cycles are a consequence of the differences in rainfall during the year and they influence a lot the water monitoring. Hydroelectric plants currently constitute an indispensable component for supplying renewable energy. However, this reservoir, as the others in the Amazon region, has had several impacts on the ecosystem: loss of biodiversity of terrestrial and aquatic fauna and flora, high concentration of organic matter in the water bottom due to vegetation inundation, chemical changes in the water downstream, large volume of anoxic water in the reservoir and downstream, loss of water quality (low dissolved oxygen, high conductivity, low pH, high content of dissolved and particulate, organic matter), high concentration of aquatic macrophytes and reduction of fisheries downstream.

The reservoir has impacted also on the human settlements in the area by weakening physical infrastructure, decreasing efficiency in land use, creating resettlement problems and influencing mining operations on the reservoir itself [99]. For these reasons, the area is of highly interest and water monitoring is one of the important things that have to be in place to ensure the sustainability of the reservoir.

The ANN training results for the monitoring of this important reservoir by sampling stations and hydrological cycle water are shown in the table 4.7, the values are considered low, mean square errors (MSE) for neural network training as follows for Chlorophyll_a, Transparency and Total Suspended Solids.
The Relative Errors were calculated by the equation (4.4) and showed in 4.9 :

$$RelativeError(E_r) = \frac{|X_e - X_o|}{X_o} \tag{4.4}$$

where:
Xe: Estimated Value
Xo: Observed Value

Figures 4.24, 4.25, 4.26 shows the validation results for 2014 for C1, C2, M1, M3, MBB, MJV and MIP sample stations, with the laboratory results being the "observed values" and those obtained by wavelet transformation of the remote sensing images and subsequent analysis by ANN, proposed herein, being the "estimated values", regarding chlorophyll-a, total suspended solids and transparency. The X-axes of figures represent the hydrological cycles (1, 2, 3 and 4, respectively, the full, emptying, dry and filling stages). The Y-axis represents the quantitative value of the analyzed parameter in a given hydrological cycle.

As the results given in table 4.8 and 4.9 show the errors between expected and observed values are quite low. In particular, the bests results were obtained during the dry season cycle 3 (September-October-November) for Total Suspended Solids. This period corresponds to the less cloudy period in the region. This facilitate the analysis based on satellite images and allows to obtain most accurate results.

In general, the errors are considered low and neural network showed good results and can aid in the evaluation of physico-chemical parameters, which in turn allows the identification of possible anthropogenic impacts, being relevant in environmental management and in political decision-making processes.

The results estimated by the method proposed in the present study, when compared with those observed in the laboratory proved extremely close to each other, demonstrating adequate efficiency of the proposed method. As the relationship between the estimated data and in-situ data is reliable, it would therefore be possible to estimate and chart the water quality of this reservoir back to the first satellite images obtained for the area, which would be interesting in order to track anthropogenic impacts rates throughout the years, from 1984 until today.

Potential sources of error when using remote sensing images can be due to varying atmospheric conditions. These include bad weather conditions, such as clouds, which affect the amount of incoming solar radiation reaching the water surface and the fraction of light leaving the water surface that reaches the satellite sensor[100]. In fact, clouds have been shown to interfere significantly in the monitoring of physico-chemical water characteristics and novel methods are being developed to surpass this issue, such as a model based on the ratio of green and blue band reflectance considering the bio-optical property of chlorophyll-a combined to ordinary kriging, which model was highly capable of predicting the chlorophyll-a concentration in regions covered by clouds and thus, effective in monitoring water quality in tropical shallow waters[101].

In addition, sun glint, the specular reflection of light from water surfaces towards the satellite sensor, is also a serious confounding factor for remote sensing of water column properties and benthos [97] .

Retrieval of information such as chlorophyll content, benthic features or bathymetry in these cases requires both high measurement sensitivity and a robust algorithm that can separate and remove the effect of glint [97]. Sun glint correction methods have been previously applied, such as use of wind speed and direction, application of neural networks [102], scaling depending on the brightest and darkest points of the images [103], use of the depth of the 760 nm oxygen absorption band [104] or methods using predictions of reflection based on water surface models (applied in operational ocean color data processing spatial resolutions of 100–1,000 m) and those that use in-scene information with the assumption of no near-infrared wavelength radiance leaving the water surface (applied to high resolution images of coral reefs and other shallow waters with pixel sizes of around 1–10 m) [29], [105].

Novel methods such as applying neural networks to separate the effects of the aerosol scattering, water-leaving radiance and glint are also being developed[97].

In the present study, slightly different values between estimated and in-situ data were observed in some cases, attributed to either the presence of clouds or sun glint in the remote sensing images, corroborating previous studies [100].

This should, thus, be taken into account when applying this type of methodology to environmental monitoring of reservoirs, even though differences were very slight, and corrections to these issues were done using the Dark Object Subtraction (DOS) method, providing better results in this research.

Even though atmospheric conditions influenced estimated and in-situ data in the present study, the proposed method is still shown to be reliable in comparison to other studies that also suffered atmospheric interferences, such as a study that evaluated the performance of images obtained from the sensor Operational Land Imager (OLI) onboard the Landsat-8 satellite in determining Chl-a concentrations and aiming at classifying a Brazilian tropical reservoir in the state of São Paulo with regard to trophic status, that showed reasonable results but impaired performance due to atmospheric influences [34].

On the other hand, the use of Support Vector Machines in conjunction with a

Radial Base function using TM/Landsat-5 time-series images showed more interesting results, albeit applied to observe differences in Land Use and Land Cover in a Hydroelectric system located between the states of Rio de Janeiro and São Paulo, also in Brazil [35].

Another study estimated the coloured dissolved organic matter absorption coefficient at 440 nm at another Brazilian reservoir in São Paulo using operational land imager (OLI)/Landsat-8 images and created distribution maps based on the adjusted algorithm. The authors of that study were able to adequately analyze this inland water body by the proposed method, but state that future research is needed to confirm if this model can be used in other reservoirs [33].

We intend to overcome these issues in this research and apply the methodology in other water reservoirs, in order to validate the proposal in a broader and concise way. This is also the case in the present study, where future studies are still required since, even though the data was very satisfactory regarding eutrophic categorization, there is no information of the application of this model in other ecosystems, which shall be the basis for future studies in order to demonstrate wider applicability.

4.3 Final Considerations

The present study demonstrated the application of wavelet Neural Network for estimating Chlorophyll-a levels, Transparency and Total Suspended Solids using concentration of the water samples collected in the Amazon reservoir. Satellite images, landsat7, ETM + sensor, band 1 (TM1), band 2 (TM2), band 3 (TM3) and band 4 (TM4) were used to train the ANN by hydrological cycle (full, emptying, dry, fillying) for 4 years.

A time series was analyzed and parameters were predicted with good acuracy considering the well-defined seasonal characteristics of the region. The method resulted in satisfactory approximations of laboratory results regarding the same water samples.

The neural network demonstrated good results between observed and estimated after Atmospheric corrections in satellites images. The ANNs showed in the results are useful to estimate these concentrations using remote sensing and wavelet transform. Therefore, the techniques proposed and applied in the present study are very importante since they can aid in evaluating important physico-chemical parameters, which, in turn, allows for identification of possible anthropogenic impacts, being relevant in environmental management and policy decision-making processes.

It is clear that the method proposed in this study is specific for reservoirs such as Tucuruí, which have well defined hydrological cycles, although nothing prevents this method from being used in the monitoring of waters of other reservoirs, which, in turn, must consider the seasonal differences from each region. Thus, the results can help in environmental monitoring by proposing a less expensive alternative in environmental decision-making processes.

This research contributes the evaluation of different methods accuracy in estimating of physico-chemical parameters, from multispectral satellite images. Future studies will be conducted regarding atmospheric interferences and corrections and different ecosystem characteristics. The method proposed allows the identification of possible anthropogenic impacts, being relevant in environmental management, in order to mitigate these impacts and attempt the recovery of degraded water bodies.

	Initial	Extraction
Turbidity	1.000	.75
Total Suspended Solids	1.000	.69
PO4	1.000	.61
NO3	1.000	.52
NH4	1.000	.69
Mg	1.000	.62
Na	1.000	.67
K	1.000	.68
Fe2	1.000	.71
Fe3	1.000	.55
Ca	1.000	.59
Chloro	1.000	.74
FeTotal	1.000	.78
Conductivity	1.000	.69
pH	1.000	.75
Dissolved Oxygen	1.000	.62
Transparency	1.000	.79
Temperature	1.000	.74
Chlorophyll	1.000	.71
PTOTAL	1.000	.83

Figure 4.1. Communalities

Component	Initial Eigenvalues			Extraction Sums of Squared Loadings			Rotation Sums of Squared Loadings		
	Total	% of Variance	Cumulative %	Total	% of Variance	Cumulative %	Total	% of Variance	Cumulative %
1	5.977	29.884	29.884	5.977	29.884	29.884	5.424	27.118	27.118
2	2.469	12.347	42.231	2.469	12.347	42.231	2.008	10.040	37.159
3	1.528	7.638	49.869	1.528	7.638	49.869	1.653	8.263	45.421
4	1.456	7.282	57.151	1.456	7.282	57.151	1.637	8.183	53.605
5	1.295	6.474	63.624	1.295	6.474	63.624	1.623	8.115	61.719
6	1.012	5.061	68.685	1.012	5.061	68.685	1.393	6.966	68.685
7	.924	4.621	73.306						
8	.869	4.347	77.654						
9	.717	3.587	81.241						
10	.709	3.544	84.785						
11	.562	2.812	87.597						
12	.461	2.307	89.904						
13	.442	2.209	92.112						
14	.376	1.878	93.990						
15	.275	1.375	95.365						
16	.261	1.304	96.669						
17	.240	1.198	97.867						
18	.189	.946	98.813						
19	.135	.674	99.487						
20	.103	.513	100.000						

Figure 4.2. Total Variance Explained

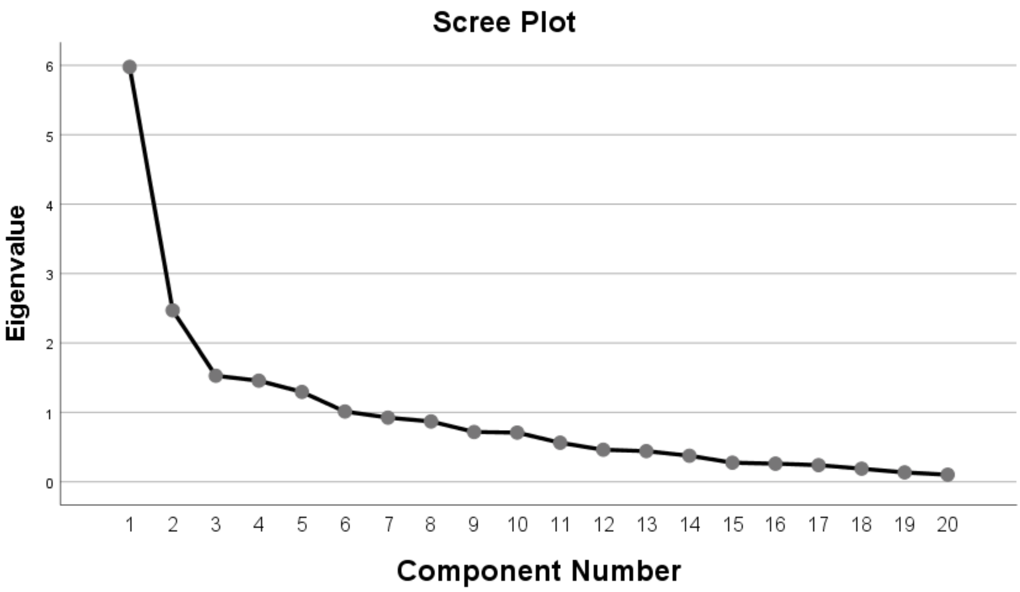

Figure 4.3. Scree Plot

	Component					
	1	2	3	4	5	6
PTOTAL	.893	.086	-.019	-.025	-.130	-.095
FeTotal	.869	.081	-.020	-.038	-.102	-.088
Turbidity	.812	-.279	-.083	.043	-.035	.031
Transparency	-.799	.033	-.038	-.014	-.278	.263
Fe2	.763	-.095	-.202	-.055	-.202	.189
Total Suspended Solids	.760	-.136	.176	.036	-.006	-.242
PO4	.733	.011	-.147	-.155	.035	-.155
Fe3	.711	.119	.001	-.086	-.070	-.116
Temperature	-.533	.374	.291	-.011	-.044	-.483
K	.378	.675	-.112	.127	-.184	.141
Na	.165	.630	-.206	.430	-.053	-.140
Cloro	.055	.521	-.445	.371	.058	.360
pH	.361	-.516	.012	.070	.413	.418
Mg	.165	.235	.693	.133	.157	.114
NH4	.322	.117	.664	.198	-.032	.309
Ca	-.174	-.471	-.061	.571	.081	-.079
Dissolved Oxygen	.090	-.463	-.156	.463	.255	-.303
Chlorophyll	.092	.445	.047	.319	.626	-.071
Conductivity	.258	.284	.045	-.510	.528	.052
NO3	.304	-.143	.364	.337	-.401	.041

Figure 4.4. Component Matrix

	Component					
	1	2	3	4	5	6
PTotal	.882	.145	.114	.089	-.094	-.052
FeTotal	.857	.133	.108	.097	-.094	-.025
Transparency	-.805	.001	-.131	-.056	-.177	-.295
Total Suspended Solids	.780	-.107	.219	.014	.136	-.003
Turbidity	.767	-.032	.045	.362	.124	-.097
PO4	.757	.036	-.080	.097	-.065	.119
Fe3	.715	.099	.086	.021	-.124	.026
Fe2	.699	.124	-.043	.388	-.133	-.193
Chloro	-.088	.826	-.096	.199	-.051	.059
Na	.155	.743	.035	-.303	.059	.029
K	.303	.667	.134	-.091	-.341	-.024
NH4	.151	.038	.799	.125	-.095	-.086
Mg	.047	.006	.761	-.087	-.069	.155
Temperature	-.379	-.031	.093	-.762	-.038	.101
pH	.185	-.202	.153	.737	.268	.181
Dissolved Oxygen	.134	-.078	-.113	.067	.759	.022
Ca	-.183	-.040	-.002	.126	.709	-.203
Conductivity	.217	-.065	.033	.090	-.376	.700
Chlorophyll	.006	.443	.255	-.096	.236	.618
NO3	.261	-.005	.434	.002	.135	-.497

Figure 4.5. Rotated Component Matrix

Component	1	2	3	4	5	6
1	.942	.122	.179	.254	-.032	.030
2	-.031	.700	.158	-.425	-.479	.271
3	-.059	-.392	.886	-.226	-.083	-.011
4	-.093	.538	.299	.004	.734	-.271
5	-.088	-.028	.079	.218	.314	.916
6	-.304	.225	.252	.810	-.353	-.116

Figure 4.6. Component Transformation Matrix

	Component					
	1	2	3	4	5	6
Turbidity	.125	-.017	-.027	.114	.057	-.062
Total Suspended Solids	.186	-.109	.063	-.165	.114	.004
PO4	.175	-.036	-.131	-.067	-.013	.078
NO3	.029	.014	.266	-.051	.065	-.368
NH4	-.079	.012	.518	.137	-.076	-.086
Mg	-.057	-.037	.487	-.018	-.019	.095
Na	.044	.364	-.024	-.191	.141	-.030
K	.018	.310	.039	-.002	-.157	-.093
Fe2	.090	.066	-.077	.195	-.117	-.160
Fe3	.156	-.008	-.021	-.095	-.047	-.003
Ca	-.038	.070	.032	.035	.431	-.092
Chloro	-.117	.479	-.054	.278	-.002	-.008
FeTotal	.173	.015	-.017	-.062	-.032	-.042
Conductivity	.017	-.114	-.008	.085	-.206	.495
pH	-.095	-.032	.128	.506	.087	.176
Dissolved Oxygen	.070	.009	-.082	-.091	.499	.080
Transparency	-.184	.062	.002	.129	-.166	-.224
Temperature	.049	-.090	.052	-.525	.067	.063
Chlorophyll	-.035	.205	.144	-.030	.248	.441
PTotal	.179	.020	-.016	-.072	-.031	-.063

Figure 4.7. Component Score Coefficient Matrix

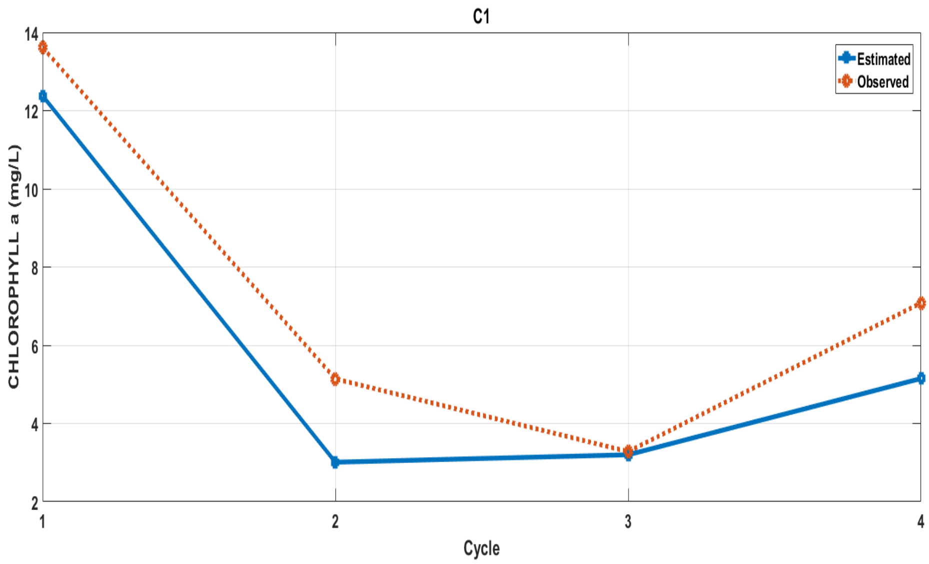

Figure 4.8. Predicting Chlorophylla in hydroelectric power plant reservoir by wavelet transformation of spectral bands for sample station: C1

Table 4.3. Approximation errors of the proposed method for 2014 per sampling station, evaluated parameter and hydrological cycle.

FULL				
Station	Variable	Error	Lab	Ann
C1	Transparency	0.2814	1.4	1.6814
	TSS	2.6139	1.33	3.9439
	Chlorophylla	5.9924	2.38	8.7924
C2	Transparency	0.2192	2.8	3.0192
	TSS	0.0823	1.4	1.3177
	Chlorophylla	0.8967	4.76	5.6567
M1	Transparency	0.5216	1.8	2.3216
	TSS	1.1455	1.6	2.7455
	Chlorophylla	6.0581	2.62	8.6781
M3	Transparency	−0.328	1.2	0.0872
	TSS	3.9784	5	8.9784
	Chlorophylla	0.8267	5.95	6.7767
MBB	Transparency	0.1356	2.2	2.3356
	TSS	−0.2081	2	1.7919
	Chlorophylla	−1.4084	3.81	2.4016
MIP	Transparency	0.0627	0.5	0.5627
	TSS	16.4403	24	40.4403
	Chlorophylla	−1.92	5.78	3.86
ML	Transparency	0.4832	1.4	1.8832
	TSS	0.1003	4.1	4.2003
	Chlorophylla	−4.678	5.155	0.477
MP	Transparency	−0.097	2.7	2.603
	TSS	1.6706	1.6	3.2706
	Chlorophylla	0.3362	6.19	6.5262
MR	Transparency	−0.2057	2.5666	2.3609
	TSS	−1.7169	2.8	1.0831
	Chlorophylla	−1.2658	8.57	7.3042

Table 4.4. Approximation errors of the proposed method for 2014 per sampling station, evaluated parameter and hydrological cycle.

Emptying				
Station	Variable	Error	Lab	Ann
C1	Transparency	0.2792	2.8	3.0792
	TSS	1.0023	1.4	2.4023
	Chlorophylla	0.6872	3.81	4.4972
C2	Transparency	−0.5621	3.45	2.8879
	TSS	0.8448	1	1.8448
	Chlorophylla	−2.5848	9.045	6.4602
M1	Transparency	0.0009	4.2	4.2009
	TSS	−0.2141	0.4	0.1859
	Chlorophylla	2.0696	1.9	3.9696
M3	Transparency	−0.4106	3	2.5894
	TSS	−0.125	1.2	1.075
	Chlorophylla	0.7833	5.47	6.2533
MBB	Transparency	−0.6815	4.3	3.6185
	TSS	0.9171	1	1.9171
	Chlorophylla	0.1938	3.57	3.7638
MIP	Transparency	−0.3955	1.9	1.5045
	TSS	5.3545	1.8	5.3345
	Chlorophylla	0.29309	3.09	6.0209
ML	Transparency	−0.5521	3.2	2.6479
	TSS	0.1969	1.4	1.5969
	Chlorophylla	1.8254	5.47	7.2954
MP	Transparency	−0.9233	2.9	1.9767
	TSS	0.7272	1.5	2.2272
	Chlorophylla	−0.1882	6.305	6.1168
MR	Transparency	−0.5146	3.066	2.552
	TSS	0.3851	1.3	1.6851
	Chlorophylla	2.478	5.83	8.308

Table 4.5. Approximation errors of the proposed method for 2014 per sampling station, evaluated parameter and hydrological cycle.

Dry				
Station	Variable	Error	Lab	Ann
C1	Transparency	−0.4642	3	2.5358
	TSS	−0.0085	1.2	1.1915
	Chlorophylla	−2.7352	4.76	2.0248
C2	Transparency	0.61	1.6	2.21
	TSS	−1.823	4	3.177
	Chlorophylla	−4.3263	12.14	7.8137
M1	Transparency	0.3704	4.2666	4.637
	TSS	−0.637	0.8	0.163
	Chlorophylla	−1.9406	1.9	−0.0406
M3	Transparency	−0.3566	2.7	2.3434
	TSS	0.7951	0.8	1.5951
	Chlorophylla	1.1384	4.76	5.8984
MBB	Transparency	1.0036	3.6	4.6036
	TSS	−0.4702	1.8	1.3298
	Chlorophylla	−0.3239	5.47	5.1461
MIP	Transparency	1.2495	1.1	2.3495
	TSS	−1.788	3.4	1.612
	Chlorophylla	−5.1001	3.81	−1.2901
ML	Transparency	0.0592	1.8	1.8592
	TSS	−0.7169	3.5	2.7831
	Chlorophylla	3.4678	9.64	113.1078
MP	Transparency	0.2012	1.9	2.1012
	TSS	3.5004	4.6	8.1004
	Chlorophylla	−1.1722	12.61	11.4378
MR	Transparency	−0.8117	2.3333	1.5216
	TSS	−0.9255	2.4	1.4745
	Chlorophylla	−1.0767	4.52	3.4433

Table 4.6. Approximation errors of the proposed method for 2014 per sampling station, evaluated parameter and hydrological cycle.

Filling				
Station	Variable	Error	Lab	Ann
C1	Transparency	−0.4097	2.8	2.3903
	TSS	2.5042	1.8	4.3042
	Chlorophylla	−1.1741	6.66	5.4859
C2	Transparency	−0.7294	1.95	1.2206
	TSS	3.5761	3.8	7.3761
	Chlorophylla	14.9382	13.39	28.3282
M1	Transparency	2.3255	1.5333	3.8558
	TSS	0.0816	2.3	2.3816
	Chlorophylla	0.1989	2.62	2.8189
M3	Transparency	−0.0499	1.3	1.2501
	TSS	−1.1787	5.2	4.0213
	Chlorophylla	1.6353	6.9	8.5353
MBB	Transparency	0.3015	1.6	1.9105
	TSS	0.0929	2.2	2.2929
	Chlorophylla	0.08846	2.86	3.7446
MIP	Transparency	−0.2286	0.8	0.5714
	TSS	12.6127	24.75	37.3627
	Chlorophylla	−1.8653	5.71	3.8447
ML	Transparency	0.0279	0.8	0.8279
	TSS	−1.0154	9.2	8.1846
	Chlorophylla	3.2846	5.95	9.2346
MP	Transparency	0.1187	0.95	1.0687
	TSS	−2.2222	8.45	6.2278
	Chlorophylla	4.0724	10.83	14.9024
MR	Transparency	−0.2366	2.5	2.2634
	TSS	−0.6972	2.5	1.8029
	Chlorophylla	2.5624	7.14	9.7024

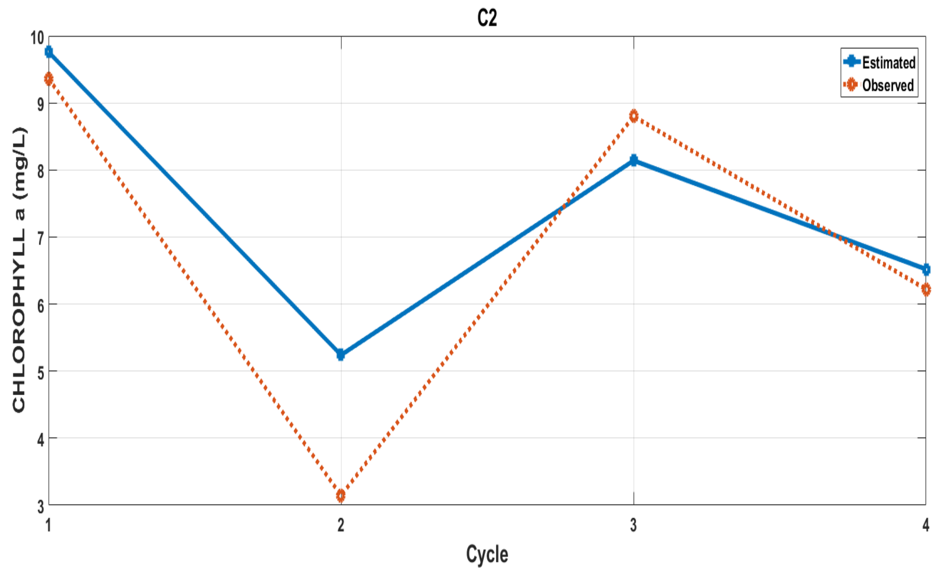

Figure 4.9. Predicting Chlorophylla in hydroelectric power plant reservoir by wavelet transformation of spectral bands for sample station: C2

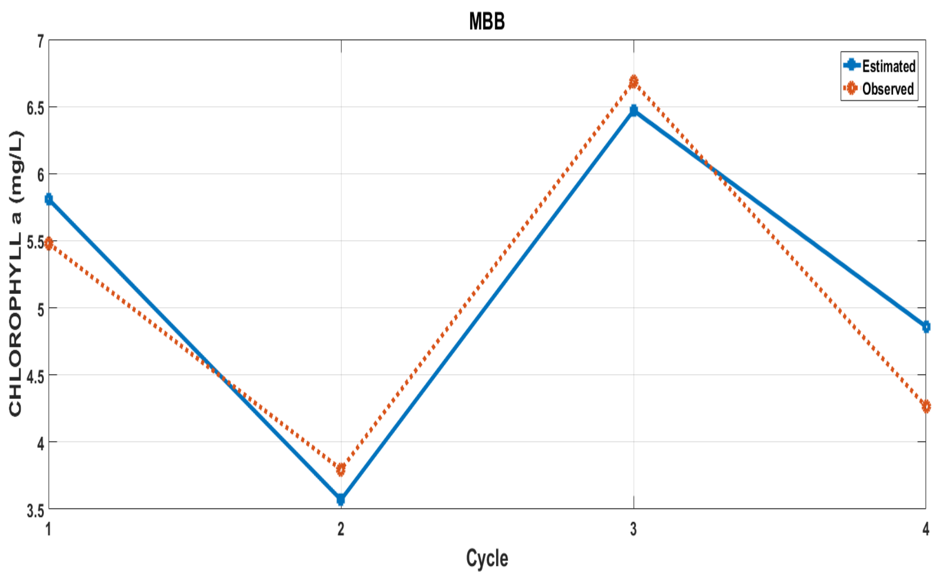

Figure 4.10. Predicting Chlorophylla in hydroelectric power plant reservoir by wavelet transformation of spectral bands for sample station: MBB

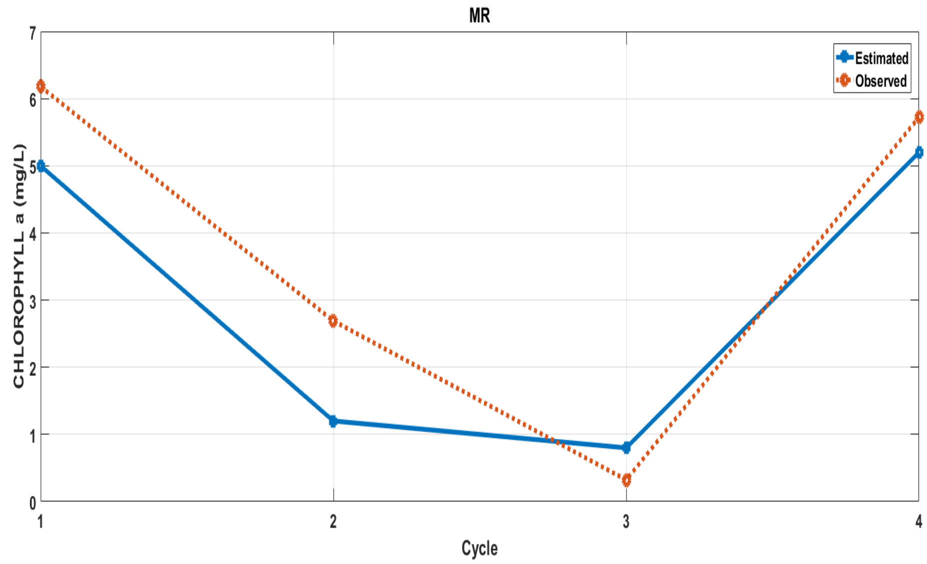

Figure 4.11. Predicting Chlorophylla in hydroelectric power plant reservoir by wavelet transformation of spectral bands for sample station: MR

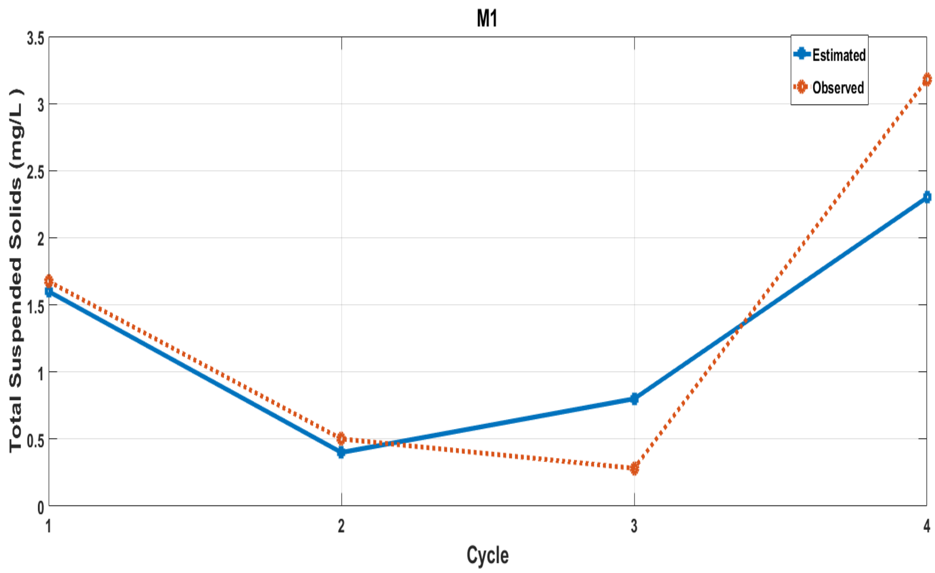

Figure 4.12. Predicting Total Suspended Solids in hydroelectric power plant reservoir by wavelet transformation of spectral bands for sample station: M1

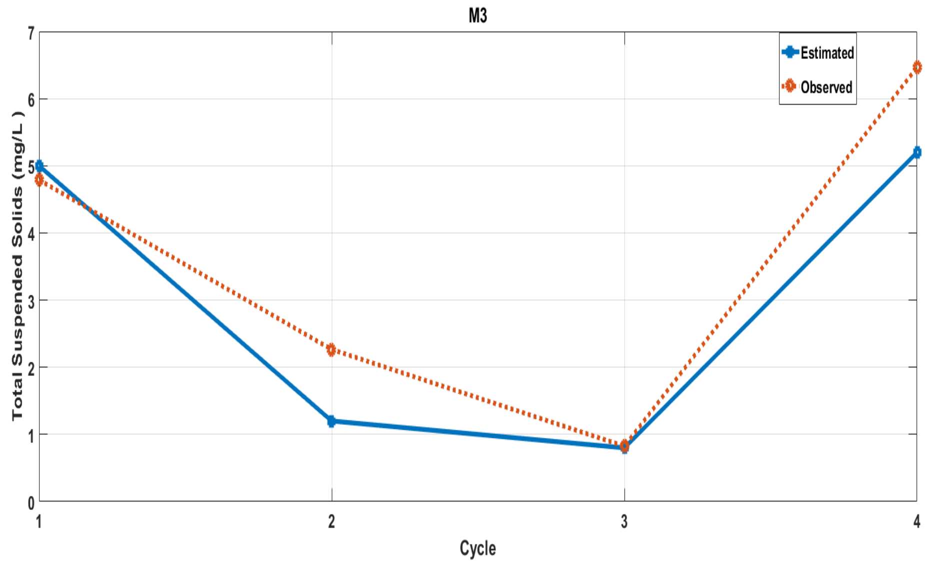

Figure 4.13. Predicting Total Suspended Solids in hydroelectric power plant reservoir by wavelet transformation of spectral bands for sample station: M3

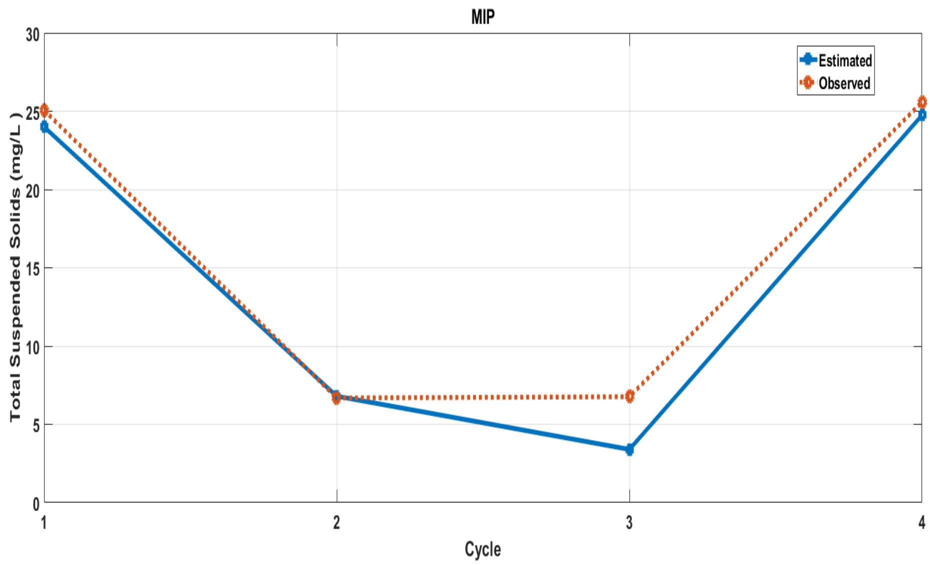

Figure 4.14. Predicting Total Suspended Solids in hydroelectric power plant reservoir by wavelet transformation of spectral bands for sample station: MIP

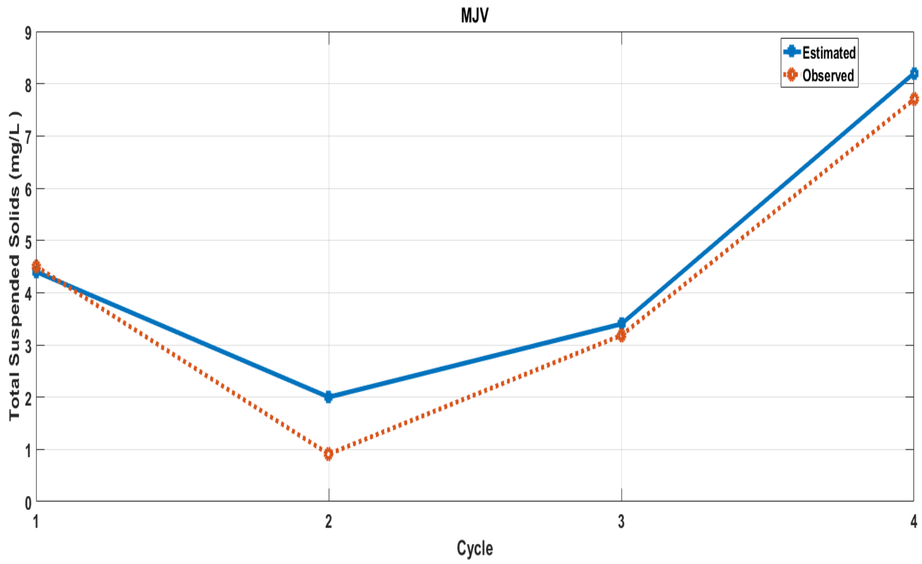

Figure 4.15. Predicting Total Suspended Solids in hydroelectric power plant reservoir by wavelet transformation of spectral bands for sample station: MJV

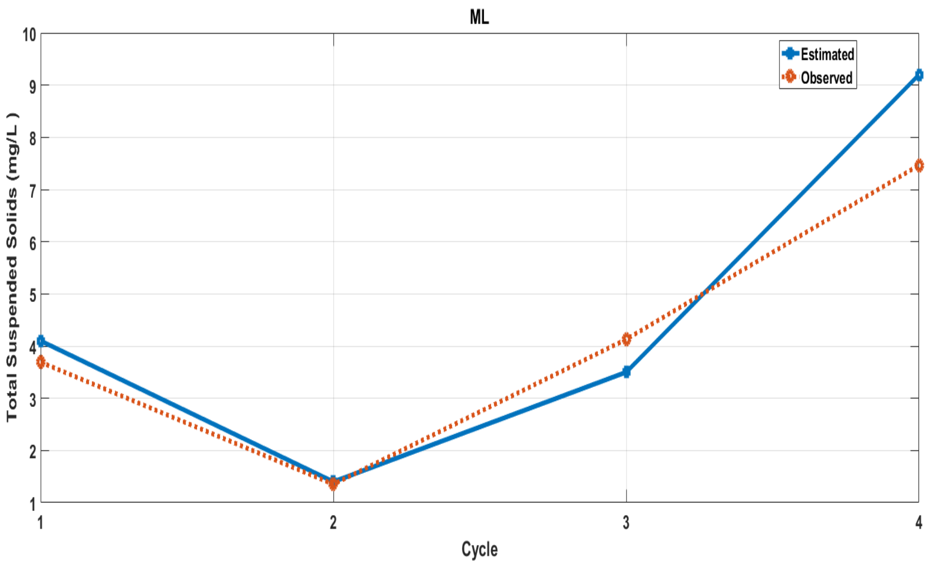

Figure 4.16. Predicting Total Suspended Solids in hydroelectric power plant reservoir by wavelet transformation of spectral bands for sample station: ML

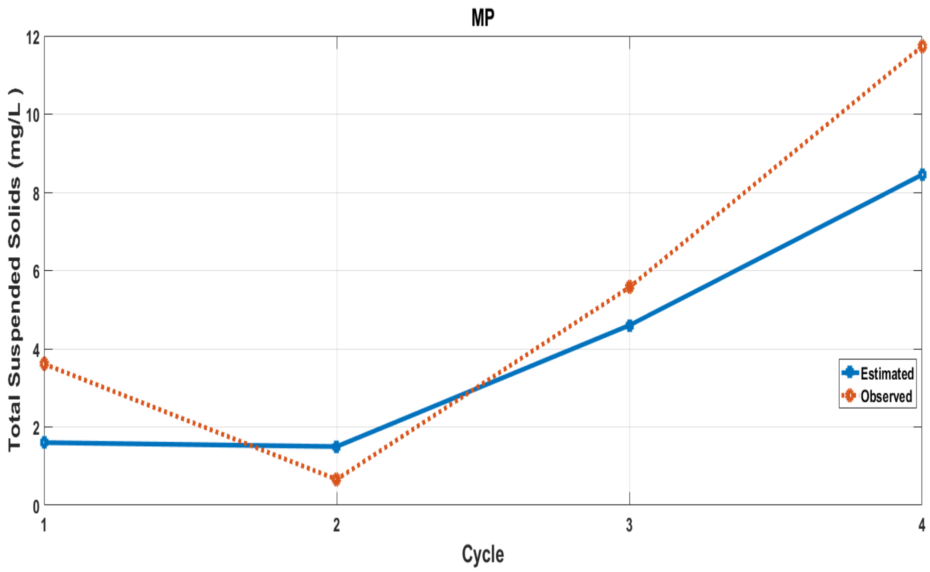

Figure 4.17. Predicting Total Suspended Solids in hydroelectric power plant reservoir by wavelet transformation of spectral bands for sample station: MP

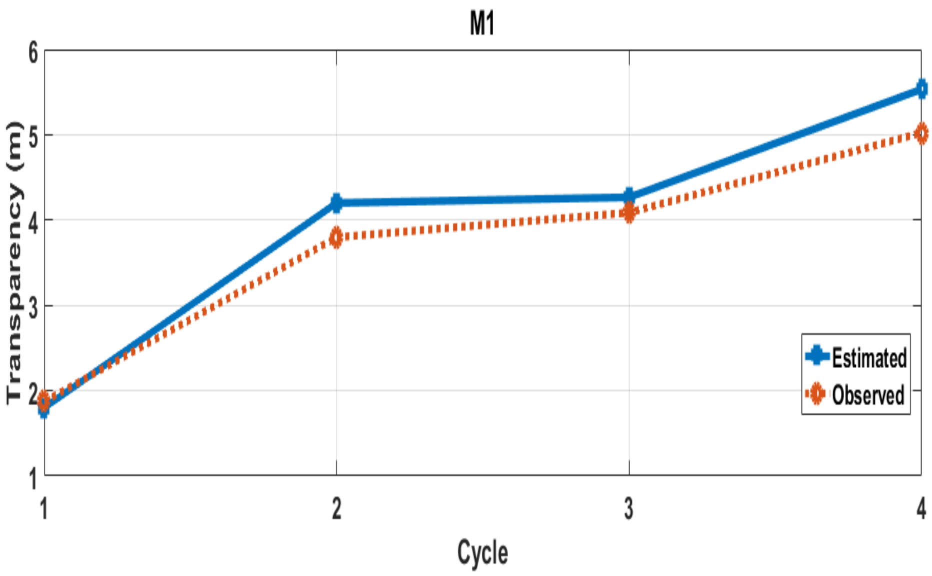

Figure 4.18. Predicting Transparency in hydroelectric power plant reservoir by wavelet transformation of spectral bands for sample station: M1

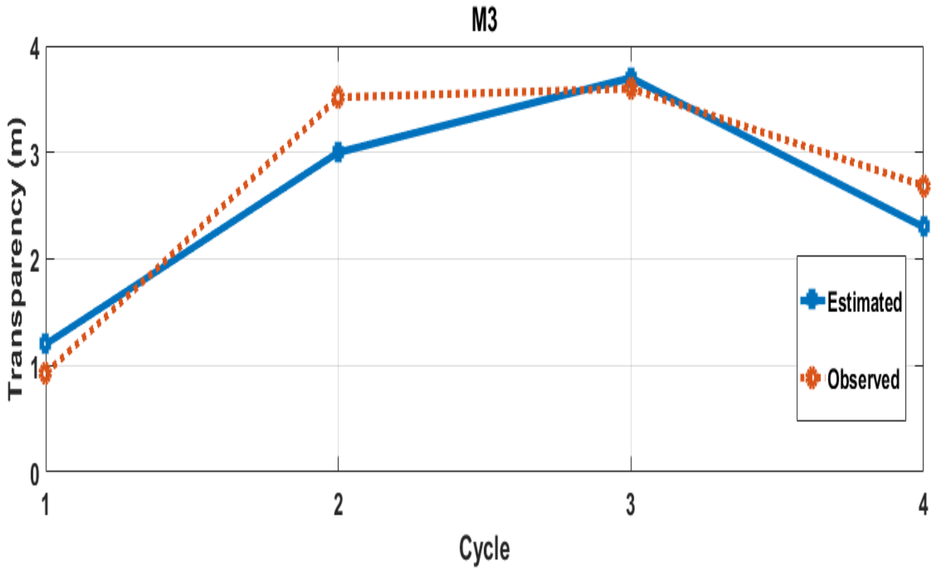

Figure 4.19. Predicting Transparency in hydroelectric power plant reservoir by wavelet transformation of spectral bands for sample station: M3

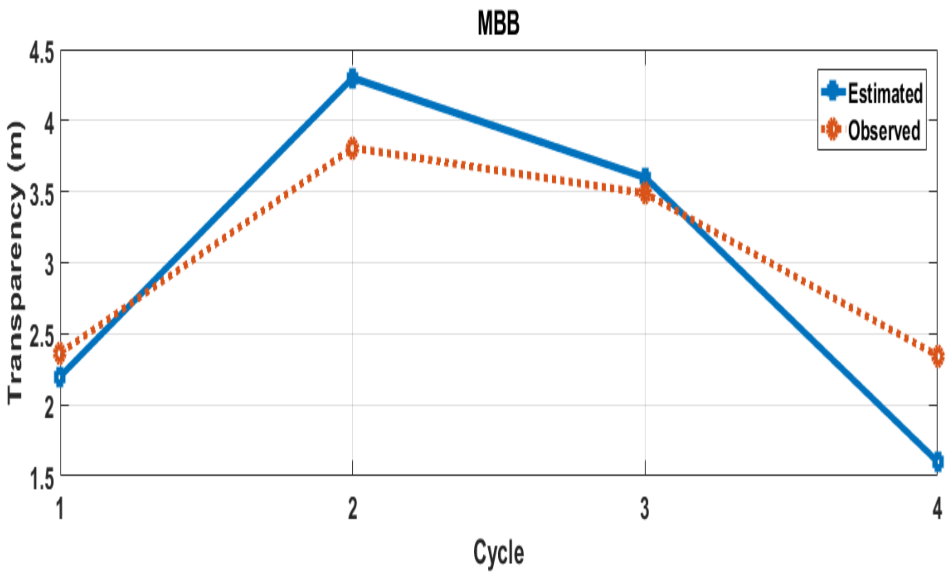

Figure 4.20. Predicting Transparency in hydroelectric power plant reservoir by wavelet transformation of spectral bands for sample station: MBB

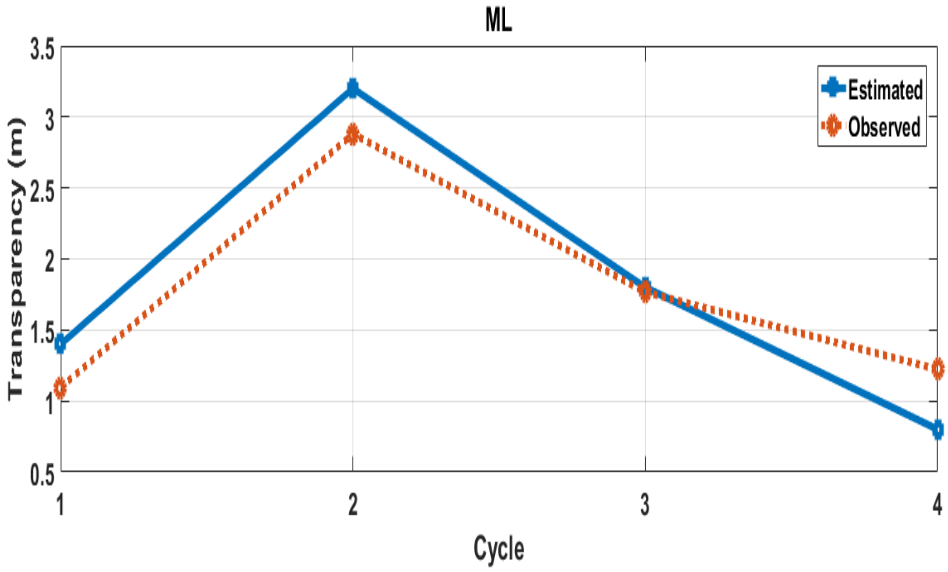

Figure 4.21. Predicting Transparency in hydroelectric power plant reservoir by wavelet transformation of spectral bands for sample station: ML

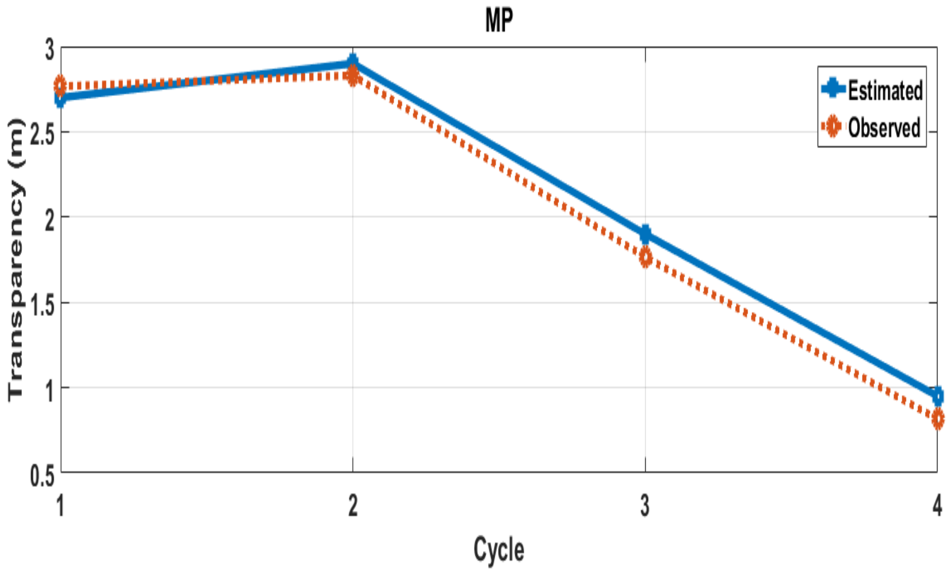

Figure 4.22. Predicting Transparency in hydroelectric power plant reservoir by wavelet transformation of spectral bands for sample station: MP

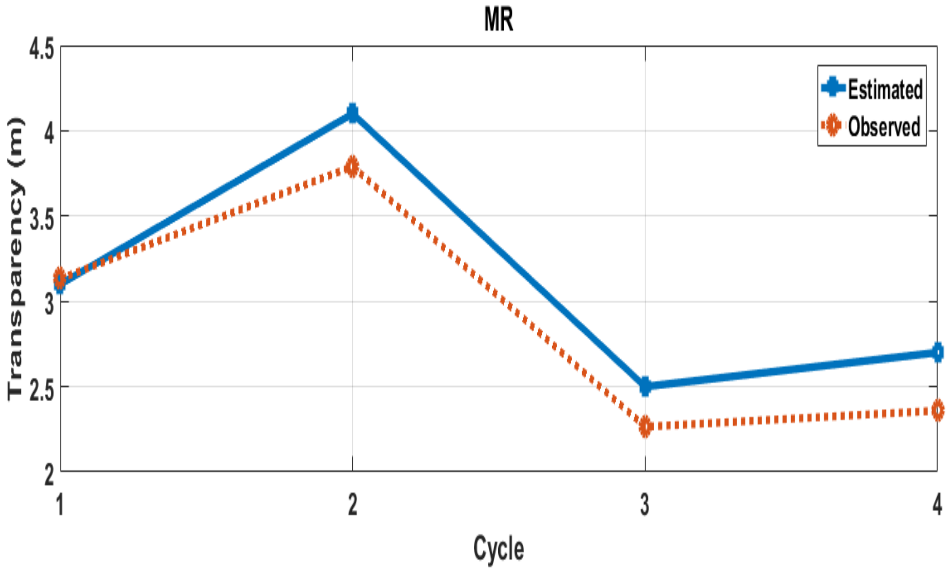

Figure 4.23. Predicting Transparency in hydroelectric power plant reservoir by wavelet transformation of spectral bands for sample station: MR

Table 4.7. Mean Square Errors (MSE) in the ANN training conducted in the present study

MSE						
Parameters	Station	Full	Emptying	Dry	Filling
CHLOROPHYLLa	C1	1.25×10^{-23}	3.70×10^{-07}	1.35×10^{-22}	6.68×10^{-24}
	C2	4.44×10^{-22}	3.97×10^{-24}	5.61×10^{-22}	2.73×10^{-07}
	MBB	1.27×10^{-22}	5.37×10^{-09}	1.33×10^{-23}	2.04×10^{-22}
TRANSPARENCY	MJV	3.78×10^{-06}	3.72×10^{-08}	2.43×10^{-22}	1.11×10^{-22}
	M1	5.39×10^{-08}	2.78×10^{-07}	5.83×10^{-07}	1.88×10^{-10}
	M3	1.14×10^{-08}	9.67×10^{-09}	3.15×10^{-22}	4.67×10^{-21}
TSS	M3	4.63×10^{-07}	2.43×10^{-08}	9.88×10^{-23}	3.83×10^{-23}
	MJV	3.10×10^{-05}	7.70×10^{-09}	1.31×10^{-21}	3.80×10^{-23}
	MIP	4.89×10^{-24}	5.06×10^{-09}	3.01×10^{-04}	1.66×10^{-22}

Table 4.8. Approximation errors for 2014 per sampling station, evaluated parameter and hydrological cycle.

MSE Validation by Cycle					
Parameters	Station	Full	Emptying	Dry	Filling
CHLOROPHYLLa	C1	1.1593	17.1529	0.2679	5.4940
	C2	0.1555	4.3905	0.4366	0.0889
	MBB	0.3346	0.0070	0.8778	0.1564
TRANSPARENCY	MJV	0.1789	0.0736	0.0156	0.0828
	M1	0.0010	0.4436	0.4957	0.0272
	M3	0.0966	0.2470	0.2272	0.2318
TSS	M3	0.0444	1.1343	0.0006	1.6069
	MJV	0.0106	1.1881	0.0471	0.2483
	MIP	1.1363	0.0135	11.3284	0.7024

Table 4.9. Relative Error (Er) per sampling station, evaluated parameter and hydrological cycle.

Relative Error					
Parameters	Station	Full	Emptying	Dry	Filling
CHLOROPHYLLa	C1	0.0800	0.5791	0.1392	0.3128
	C2	0.0421	0.6663	0.0751	0.0479
	MBB	0.1106	0.0229	0.2067	0.0886
TRANSPARENCY	MJV	0.4824	0.0979	0.0793	0.2423
	M1	0.0180	0.1885	0.1416	0.0307
	M3	0.3495	0.1421	0.1479	0.1731
TSS	M3	0.0440	0.4702	0.0303	0.1960
	MJV	0.0229	1.1978	0.0682	0.0647
	MIP	0.0425	0.0174	0.4975	0.0328

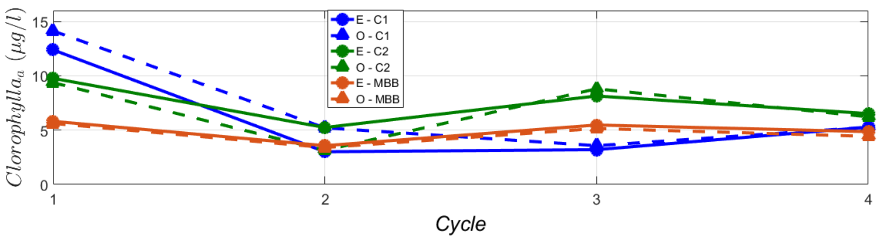

Figure 4.24. Predicting Chlorophyll_a Levels in hydroelectric power plant reservoir by wavelet transformation of spectral bands for sample station: C1 - Caraipé 1, C2 - Caraipé 2, MBB - Breu Branco; E = Estimated; O = Observed

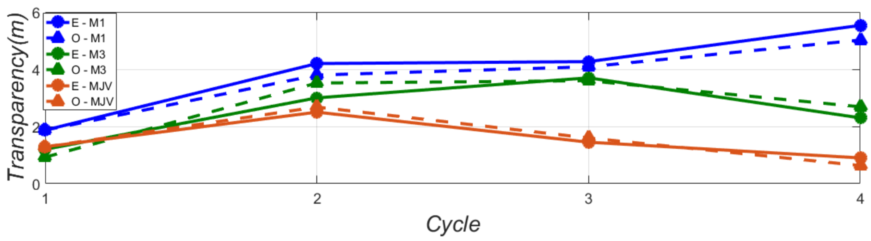

Figure 4.25. Predicting Transparency in hydroelectric power plant reservoir by wavelet transformation of spectral bands for sample station: M1 - Upstrem 1, M3 - Upstrem 3 , MJV - Jacunda Velho; E = Estimated; O = Observed

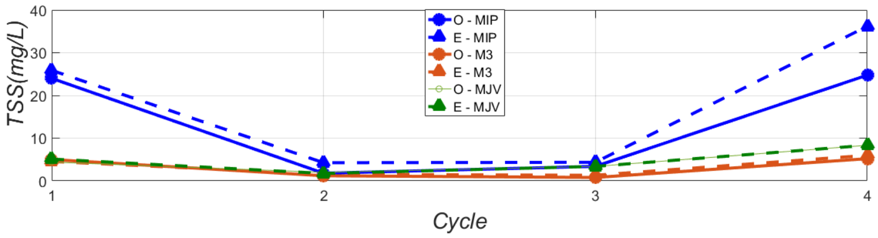

Figure 4.26. Predicting Total Suspended Solids in hydroelectric power plant reservoir by wavelet transformation of spectral bands for sample station: MIP - Ipixuna , M3 - Upstrem 3 , MJV - Jacunda Velho; E = Estimated; O = Observed

Chapter 5

Conclusions and Future Works

This study demonstrated the application of virtual sensors in the estimation of the physico-chemical parameters in water bodies using satellite images of spectral band 1, band 2, band 3 and band 4 that has sensitivity to the presence of particulate matter in water bodies.

The factorial analysis confirmed the correlation between the physico-chemical parameters in the first depth of the Secchi disc, PTotal, FeTotal, Turbidity, Transparency, Fe2, Total Suspended Solids, PO4, Fe2 and Fe3 were related to Factor 1, since these present great reflectance and good absorption of energy by the sensors of the satellites.

The wavelet Neural Network was trained receiving as input a pixel vector of the satellite images. One sampling station was initially chosen for analysis and an image of the water sampling point 32x32 pixels was cropped, corresponding to an array containing 1024 pixels.

Subsequently, the wavelet transform was applied, with only one level of decomposition, resulting in a matrix array of 16x16 pixels for each of the following three components: Horizontal (H), vertical (V) and diagonal (D).

The conversion of the arrays to the H, V and D components to their respective column-matrices was performed, and subsequently a concatenation of the three arrays (each containing 256 pixels) was executed, generating a vector with 768 column size (256 x 3). This data, the image of the water sampling collection point, decomposed via wavelet into its three wavelet components, was used as the ANN input.

Tests were conducted considering the image representations isolated for each wavelet component, with satisfactory results. However, when the input data of the three wavelet components was considered, the approximations were even better, which motivated the choice of this arrangement in the proposed solution.

Some collection stations could not be analyzed due to the low number of data available in the database. However, the results obtained showed that method for predicting chlorophyll-a levels, transparency and total suspended solids in the Tucuruí reservoir have sensitivity to the presence of suspended particulate matter with satisfactory approximations of laboratory results regarding the same water samples.

For the collection points that were analyzed the ANN showed to be useful for estimating physico-chemical parameters, producing satisfactory results with good approximation between the observed and estimated values.

In general, the errors are considered low and neural network showed good results and can aid in the evaluation of physico-chemical parameters, which in turn allows the identification of possible anthropogenic impacts, being relevant in environmental management and in political decision-making processes.

The bests results were obtained during the dry season cycle 3, (September-October-November), for Total Suspended Solids, Chlorophylla and Transparency parameters. The dry period has few clouds in the region, allowing a good analysis of satellite images.

It is clear that the proposed method in this study is specific to the Tucuruí hydroelectric power plant reservoir waters, although nothing prevents this method to be used in monitoring waters from other reservoirs, as we intend to do in the Cefni reservoir, which in turn should result in less expenditures on environmental monitoring processes.

The techniques proposed and applied in the present study can aid in evaluating important physico-chemical parameters, which, in turn, allows for identification of possible anthropogenic impacts, being relevant in environmental management and policy decision-making processes, in order to mitigate these impacts and attempt the recovery of degraded water bodies.

In this research a model was proposed using virtual sensors in the estimation of Physico-Chemical Parameters: Secchi Disk Depths (SD), PTotal, FeTotal, Turbidity, Transparency, Fe2, Total Suspended Solids, PO4, Fe3, Temperature and Chorophylla_a using wavelet Artificil Neural Network and Remote Sensing in the first depth range of the secchi disk.

As a future work, it is proposed to apply other computational techniques to evaluate water quality parameters, as well as to evaluate other physicochemical parameters, verifying and estimating the concentrations of these elements in surface reflectance.

Another possibility of future work in the Tucurui reservoir is the development of a software that can allocate the collection stations according to the representativity of the concentrations of the physico-chemical parameters by means of satellite images and clustering techniques, addressing techniques of the statistical and computational intelligence.

The method proposed can be applied to other ecosystems that also suffer well-defined hydrological cycle, with worldwide relevance, after conducting investigations on atmospheric interferences and corrections and different ecosystem characteristics.

Bibliography

[1] A. Kabata-Pendias, *Trace elements in soils and plants.* CRC press, 2010.

[2] O. E. Atobatele and O. A. Ugwumba, "Seasonal variation in the physicochemistry of a small tropical reservoir (aiba reservoir, iwo, osun, nigeria)," *African Journal of Biotechnology*, vol. 7, no. 12, 2008.

[3] M. W. Song, P. Huang, F. Li, H. Zhang, K. Z. Xie, X. H. Wang, and G. X. He, "Water quality of a tributary of the pearl river, the beijiang, southern china: implications from multivariate statistical analyses," *Environmental monitoring and assessment*, vol. 172, no. 1, pp. 589–603, 2011.

[4] F. Yenilmez, F. Keskin, and A. Aksoy, "Water quality trend analysis in eymir lake, ankara," *Physics and Chemistry of the Earth, Parts A/B/C*, vol. 36, no. 5, pp. 135–140, 2011.

[5] R. Nazir, M. Khan, M. Masab, H. U. Rehman, N. U. Rauf, S. Shahab, N. Ameer, M. Sajed, M. Ullah, M. Rafeeq *et al.*, "Accumulation of heavy metals (ni, cu, cd, cr, pb, zn, fe) in the soil, water and plants and analysis of physico-chemical parameters of soil and water collected from tanda dam kohat," *Journal of Pharmaceutical Sciences and Research*, vol. 7, no. 3, pp. 89–97, 2015.

[6] J. Delgado, J. L. Cereijo-Arango, D. García-Morrondo, C. Cillero-Castro, A. Muñoz-Ibáñez, and R. Juncosa-Rivera, "Physical and chemical limnology of the abegondo-cecebre reservoir, a coruña, nw spain," in *EGU General Assembly Conference Abstracts*, vol. 18, 2016, p. 14201.

[7] B. Gülcü-Gür and S. Tekin-Özan, "The investigation of heavy metal levels in water and sediment from işikli lake (turkey) in relation to seasons and physico-chemical parameters," 2017.

[8] Y. Cavalcante, R. Hauser-Davis, A. Saraiva, I. Brandão, T. Oliveira, and A. Silveira, "Metal and physico-chemical variations at a hydroelectric reservoir analyzed by multivariate analyses and artificial neural networks: Environmental management and policy/decision-making tools," *Science of the Total Environment*, vol. 442, pp. 509–514, 2013.

[9] F. A. Prado, S. Athayde, J. Mossa, S. Bohlman, F. Leite, and A. Oliver-Smith, "How much is enough? an integrated examination of energy security, economic growth and climate change related to hydropower expansion in

brazil," *Renewable and Sustainable Energy Reviews*, vol. 53, pp. 1132–1136, 2016.

[10] B. Petroleum, "Bp energy outlook 2030. 2012."

[11] "Aneel.agência nacional de energia elétrica banco de dados de geração 2014," http://<www.aneel.gov.br/, acessed in 15/08/2018.

[12] J. C. Derisio, *Introdução ao control de poluição ambiental.* Oficina de Textos, 2016.

[13] J. G. Tundisi and T. M. Tundisi, *Limnologia.* Oficina de textos, 2016.

[14] F. A. Khan and A. A. Ansari, "Eutrophication: an ecological vision," *The botanical review*, vol. 71, no. 4, pp. 449–482, 2005.

[15] A. O. Olaniran, K. Naicker, and B. Pillay, "Assessment of physico-chemical qualities and heavy metal concentrations of umgeni and umdloti rivers in durban, south africa," *Environmental monitoring and assessment*, vol. 186, no. 4, pp. 2629–2639, 2014.

[16] S. D. P. Yadav, K. Mishra, N. K. Chaudhary, and P. Mishra, "Assessing physico-chemical parameters of potable water in dhankuta municipality of nepal," *Science*, vol. 3, no. 2, pp. 17–21, 2015.

[17] F. Soltani, R. Kerachian, and E. Shirangi, "Developing operating rules for reservoirs considering the water quality issues: Application of anfis-based surrogate models," *Expert Systems with Applications*, vol. 37, no. 9, pp. 6639–6645, 2010.

[18] A. A. Najah, A. El-Shafie, O. A. Karim, and O. Jaafar, "Water quality prediction model utilizing integrated wavelet-anfis model with cross-validation," *Neural Computing and Applications*, vol. 21, no. 5, pp. 833–841, 2012.

[19] A. Najah, A. El-Shafie, O. A. Karim, and A. H. El-Shafie, "Performance of anfis versus mlp-nn dissolved oxygen prediction models in water quality monitoring," *Environmental Science and Pollution Research*, vol. 21, no. 3, pp. 1658–1670, 2014.

[20] M. Bonansea, M. C. Rodriguez, L. Pinotti, and S. Ferrero, "Using multi-temporal landsat imagery and linear mixed models for assessing water quality parameters in río tercero reservoir (argentina)," *Remote Sensing of Environment*, vol. 158, pp. 28–41, 2015.

[21] M. Bonansea and R. Fernandez, "Remote sensing of suspended solids concentration in a reservoir with frequent wildland fires on its watershed," *Water Science and Technology*, vol. 67, no. 1, pp. 217–223, 2012.

[22] N. Karakaya, F. Evrendilek, G. Aslan, K. Gungor, and D. Karakas, "Monitoring of lake water quality along with trophic gradient using landsat data," 2012.

[23] B. R. Neto, R. Hauser-Davis, T. Lobato, A. Saraiva, I. Brandão, T. Oliveira, and A. Silveira, "Estimating physicochemical parameters and metal concentrations in hydroelectric reservoirs by virtual sensors: A case study in the amazon region," *Computer Science and Engineering*, vol. 4, no. 2, pp. 43–53, 2014.

[24] E. Tebbs, J. Remedios, and D. Harper, "Remote sensing of chlorophyll-a as a measure of cyanobacterial biomass in lake bogoria, a hypertrophic, saline–alkaline, flamingo lake, using landsat etm+," *Remote Sensing of Environment*, vol. 135, pp. 92–106, 2013.

[25] P. L. Brezonik, L. G. Olmanson, J. C. Finlay, and M. E. Bauer, "Factors affecting the measurement of cdom by remote sensing of optically complex inland waters," *Remote Sensing of Environment*, vol. 157, pp. 199–215, 2015.

[26] L. Cai, D. Tang, and C. Li, "An investigation of spatial variation of suspended sediment concentration induced by a bay bridge based on landsat tm and oli data," *Advances in Space Research*, vol. 56, no. 2, pp. 293–303, 2015.

[27] X. Giam and J. D. Olden, "Quantifying variable importance in a multimodel inference framework," *Methods in Ecology and Evolution*, 2015.

[28] L. G. Olmanson, P. L. Brezonik, J. C. Finlay, and M. E. Bauer, "Comparison of landsat 8 and landsat 7 for regional measurements of cdom and water clarity in lakes," *Remote Sensing of Environment*, 2016.

[29] B. A. Franz, S. W. Bailey, N. Kuring, and P. J. Werdell, "Ocean color measurements with the operational land imager on landsat-8: implementation and evaluation in seadas," *Journal of Applied Remote Sensing*, vol. 9, no. 1, pp. 096 070–096 070, 2015.

[30] W. Zhu and Q. Yu, "Inversion of chromophoric dissolved organic matter from eo-1 hyperion imagery for turbid estuarine and coastal waters," *IEEE Transactions on Geoscience and Remote Sensing*, vol. 51, no. 6, pp. 3286–3298, 2013.

[31] T. Dube, O. Mutanga, K. Seutloali, S. Adelabu, and C. Shoko, "Water quality monitoring in sub-saharan african lakes: a review of remote sensing applications," *African Journal of Aquatic Science*, vol. 40, no. 1, pp. 1–7, 2015.

[32] T. Rajaee and S. Khani, "Comment on "performance of anfis versus mlp-nn dissolved oxygen prediction models in water quality monitoring a. najah & a. el-shafie & oa karim & amr h. el-shafie. environ sci pollut res (2014) 21: 1658-1670"," *Environmental Science and Pollution Research*, vol. 23, no. 1, pp. 938–940, 2016.

[33] E. Alcântara, N. Bernardo, F. Watanabe, T. Rodrigues, L. Rotta, A. Carmo, M. Shimabukuro, S. Gonçalves, and N. Imai, "Estimating the cdom absorption coefficient in tropical inland waters using oli/landsat-8 images," *Remote Sensing Letters*, vol. 7, no. 7, pp. 661–670, 2016.

[34] F. S. Y. Watanabe, E. Alcântara, T. W. P. Rodrigues, N. N. Imai, C. C. F. Barbosa, and L. H. d. S. Rotta, "Estimation of chlorophyll-a concentration and the trophic state of the barra bonita hydroelectric reservoir using oli/landsat-8 images," *International journal of environmental research and public health*, vol. 12, no. 9, pp. 10 391–10 417, 2015.

[35] S. Martins, N. Bernardo, I. Ogashawara, and E. Alcantara, "Support vector machine algorithm optimal parameterization for change detection mapping in funil hydroelectric reservoir (rio de janeiro state, brazil)," *Modeling Earth Systems and Environment*, vol. 2, no. 3, p. 138, 2016.

[36] C. Doña, J. M. Sánchez, V. Caselles, J. A. Domínguez, and A. Camacho, "Empirical relationships for monitoring water quality of lakes and reservoirs through multispectral images," *IEEE Journal of Selected Topics in Applied Earth Observations and Remote Sensing*, vol. 7, no. 5, pp. 1632–1641, 2014.

[37] E. Kaneko, H. Aoki, and M. Tsukada, "Image-based path radiance estimation guided by physical model," in *Geoscience and Remote Sensing Symposium (IGARSS), 2016 IEEE International.* IEEE, 2016, pp. 6942–6945.

[38] T. Blakey, A. Melesse, M. C. Sukop, G. Tachiev, D. Whitman, and F. Miralles-Wilhelm, "Developing benthic class specific, chlorophyll-a retrieving algorithms for optically-shallow water using seawifs," *Sensors*, vol. 16, no. 10, p. 1749, 2016.

[39] G. Lantzanakis, Z. Mitraka, and N. Chrysoulakis, "Comparison of physically and image based atmospheric correction methods for sentinel-2 satellite imagery," in *Perspectives on Atmospheric Sciences.* Springer, 2017, pp. 255–261.

[40] L. Shi, Z. Mao, P. Chen, S. Han, F. Gong, and Q. Zhu, "Comparison and evaluation of atmospheric correction algorithms of quac, dos and flaash for hico hyperspectral imagery," in *SPIE Remote Sensing.* International Society for Optics and Photonics, 2016, pp. 999 917–999 917.

[41] M. Nazeer and J. E. Nichol, "Selection of atmospheric correction method and estimation of chlorophyll-a (chl-a) in coastal waters of hong kong," in *Earth Observation and Remote Sensing Applications (EORSA), 2014 3rd International Workshop on.* IEEE, 2014, pp. 374–378.

[42] N. Bernardo, F. Watanabe, T. Rodrigues, and E. Alcântara, "Atmospheric correction issues for retrieving total suspended matter concentrations in inland waters using oli/landsat-8 image," *Advances in Space Research*, 2017.

[43] L. Congedo, "Semi-automatic classification plugin for qgis," 2013.

[44] L. Congedo, L. Sallustio, M. Munafò, M. Ottaviano, D. Tonti, and M. Marchetti, "Copernicus high-resolution layers for land cover classification in italy," *Journal of Maps*, vol. 12, no. 5, pp. 1195–1205, 2016.

[45] G. Chander, B. L. Markham, and D. L. Helder, "Summary of current radiometric calibration coefficients for landsat mss, tm, etm+, and eo-1 ali sensors," *Remote sensing of environment*, vol. 113, no. 5, pp. 893–903, 2009.

[46] S. N. Goward, P. E. Davis, D. Fleming, L. Miller, and J. R. Townshend, "Empirical comparison of landsat 7 and ikonos multispectral measurements for selected earth observation system (eos) validation sites," *Remote Sensing of Environment*, vol. 88, no. 1, pp. 80–99, 2003.

[47] R. R. Irish, "Landsat 7 science data users handbook," *National Aeronautics and Space Administration, Report*, vol. 2000, pp. 415–430, 2000.

[48] A. C. Teodoro, F. Veloso-Gomes, and H. Goncalves, "Retrieving tsm concentration from multispectral satellite data by multiple regression and artificial neural networks," *IEEE Transactions on Geoscience and Remote Sensing*, vol. 45, no. 5, pp. 1342–1350, 2007.

[49] A. Elzwayie, A. El-shafie, Z. M. Yaseen, H. A. Afan, and M. F. Allawi, "Rbfnn-based model for heavy metal prediction for different climatic and pollution conditions," *Neural Computing and Applications*, pp. 1–13, 2016.

[50] J.-W. Choi, J.-H. Han, C.-S. Park, D.-G. Ko, H.-I. Kang, J. Y. Kim, Y.-J. Yun, H.-H. Kwon, and K.-G. An, "Nutrients and sestonic chlorophyll dynamics in asian lotic ecosystems and ecological stream health in relation to land-use patterns and water chemistry," *Ecological Engineering*, vol. 79, pp. 15–31, 2015.

[51] V. Kumar, A. Sharma, A. Chawla, R. Bhardwaj, and A. K. Thukral, "Water quality assessment of river beas, india, using multivariate and remote sensing techniques," *Environmental monitoring and assessment*, vol. 188, no. 3, p. 137, 2016.

[52] V. Markogianni, E. Dimitriou, and I. Karaouzas, "Water quality monitoring and assessment of an urban mediterranean lake facilitated by remote sensing applications," *Environmental monitoring and assessment*, vol. 186, no. 8, pp. 5009–5026, 2014.

[53] N. T. B. Phuong, V. P. D. Tri, N. B. Duy, N. C. Nghiem *et al.*, "Remote sensing for monitoring surface water quality in the vietnamese mekong delta: The application for estimating chemical oxygen demand in river reaches in binh dai, ben tre," *VIETNAM JOURNAL OF EARTH SCIENCES*, vol. 39, no. 3, pp. 256–268, 2017.

[54] L. Chen, M. Jamal, C. Tan, and B. Alabbadi, "A study of applying genetic algorithm to predict reservoir water quality," *International Journal of Modeling and Optimization*, vol. 7, no. 2, p. 98, 2017.

[55] F. Halal, P. Pedrocca, T. Hirose, A.-M. Cretu, and M. B. Zaremba, "Remote-sensing based adaptive path planning for an aquatic platform to monitor water quality," in *Robotic and Sensors Environments (ROSE), 2014 IEEE International Symposium on.* IEEE, 2014, pp. 43–48.

[56] E. Sharaf El Din, Y. Zhang, and A. Suliman, "Mapping concentrations of surface water quality parameters using a novel remote sensing and artificial

intelligence framework," *International Journal of Remote Sensing*, vol. 38, no. 4, pp. 1023–1042, 2017.

[57] C. Doña, N.-B. Chang, V. Caselles, J. M. Sánchez, A. Camacho, J. Delegido, and B. W. Vannah, "Integrated satellite data fusion and mining for monitoring lake water quality status of the albufera de valencia in spain," *Journal of environmental management*, vol. 151, pp. 416–426, 2015.

[58] N.-B. Chang, S. Imen, and B. Vannah, "Remote sensing for monitoring surface water quality status and ecosystem state in relation to the nutrient cycle: A 40-year perspective," *Critical Reviews in Environmental Science and Technology*, vol. 45, no. 2, pp. 101–166, 2015.

[59] Z. Yang, M. Reiter, and N. Munyei, "Estimation of chlorophyll-a concentrations in diverse water bodies using ratio-based nir/red indices," *Remote Sensing Applications: Society and Environment*, vol. 6, pp. 52–58, 2017.

[60] Y. Liu, M. A. Islam, and J. Gao, "Quantification of shallow water quality parameters by means of remote sensing," *Progress in physical geography*, vol. 27, no. 1, pp. 24–43, 2003.

[61] H. Jiao, Y. Zha, J. Gao, Y. Li, Y. Wei, and J. Huang, "Estimation of chlorophyll-a concentration in lake tai, china using in situ hyperspectral data," *International Journal of Remote Sensing*, vol. 27, no. 19, pp. 4267–4276, 2006.

[62] J. P. Cannizzaro and K. L. Carder, "Estimating chlorophyll a concentrations from remote-sensing reflectance in optically shallow waters," *Remote Sensing of Environment*, vol. 101, no. 1, pp. 13–24, 2006.

[63] N. Usali and M. H. Ismail, "Use of remote sensing and gis in monitoring water quality," *Journal of sustainable development*, vol. 3, no. 3, p. 228, 2010.

[64] X.-G. Xing, D.-Z. Zhao, Y.-G. Liu, J.-H. Yang, P. Xiu, and L. Wang, "An overview of remote sensing of chlorophyll fluorescence," *Ocean Science Journal*, vol. 42, no. 1, pp. 49–59, 2007.

[65] E. Robert, M. Grippa, L. Kergoat, S. Pinet, L. Gal, G. Cochonneau, and J.-M. Martinez, "Monitoring water turbidity and surface suspended sediment concentration of the bagre reservoir (burkina faso) using modis and field reflectance data," *International Journal of Applied Earth Observation and Geoinformation*, vol. 52, pp. 243–251, 2016.

[66] R. W. Gentry, J. McCarthy, A. Layton, L. D. McKay, D. Williams, S. R. Koirala, and G. S. Sayler, "Loading at or near base flow in a mixed-use watershed," *Journal of environmental quality*, vol. 35, no. 6, pp. 2244–2249, 2006.

[67] S. J. Giovannoni, J. C. Thrash, and B. Temperton, "Implications of streamlining theory for microbial ecology," *The ISME journal*, vol. 8, no. 8, p. 1553, 2014.

[68] P. Galès and B. Baleux, “Influence of the drainage basin input on a pathogenic bacteria (salmonella) contamination of a mediterranean lagoon (the thau lagoon-france) and the survival of this bacteria in brackish water,” *Water Science and Technology*, vol. 25, no. 12, pp. 105–114, 1992.

[69] J. van der Bliek, P. G. McCornick, and J. Clarke, *On target for people and planet: setting and achieving water-related sustainable development goals*. IWMI, 2014.

[70] B. d. Mérona, A. Juras, G. Mendes Dos Santos, and I. Cintra, “Os peixes ea pesca no baixo rio tocantins: vinte anos depois da uhe tucuruí,” 2010.

[71] T. Lobato, R. Hauser-Davis, T. Oliveira, A. Silveira, H. Silva, M. Tavares, and A. Saraiva, “Construction of a novel water quality index and quality indicator for reservoir water quality evaluation: A case study in the amazon region,” *Journal of hydrology*, vol. 522, pp. 674–683, 2015.

[72] R. Deus, D. Brito, M. Mateus, I. Kenov, A. Fornaro, R. Neves, and C. Alves, “Impact evaluation of a pisciculture in the tucuruí reservoir (pará, brazil) using a two-dimensional water quality model,” *Journal of hydrology*, vol. 487, pp. 1–12, 2013.

[73] T. Malthus and D. George, “Airborne remote sensing of macrophytes in cefni reservoir, anglesey, uk,” *Aquatic Botany*, vol. 58, no. 3-4, pp. 317–332, 1997.

[74] P. da Silva Holanda, C. J. C. Blanco, A. L. A. Mesquita, A. C. P. B. Junior, N. M. de Figueiredo, E. N. Macêdo, and Y. Secretan, “Assessment of hydrokinetic energy resources downstream of hydropower plants,” *Renewable Energy*, vol. 101, pp. 1203–1214, 2017.

[75] E. Espíndola, T. Matsumura-Tundisi, A. Rietzler, and J. Tundisi, “Spatial heterogeneity of the tucuruí reservoir (state of pará, amazonia, brazil) and the distribution of zooplanktonic species,” *Revista Brasileira de Biologia*, vol. 60, no. 2, pp. 179–194, 2000.

[76] D. Tomassi, D. Milone, and J. D. Nelson, “Wavelet shrinkage using adaptive structured sparsity constraints,” *Signal Processing*, vol. 106, pp. 73–87, 2015.

[77] J. M. B. Protázio, “Spatial pattern analysis applied to plant ecology,” Ph.D. dissertation, University of Bremen, 2007.

[78] S. Mallat, *A wavelet tour of signal processing: the sparse way*. Academic press, 2008.

[79] M. Matworks, “Neural network toolbox user’s guide: for use with matlab,” 2009.

[80] S. Karthick, S. Aanand, A. Srinivasan, and P. Jawahar, “Assessment of seasonal variations in water quality parameters of kadamba tank in thoothukudi district of tamil nadu, india,” *IJAR*, vol. 2, no. 11, pp. 329–334, 2016.

[81] C. E. Boyd, "ph, carbon dioxide, and alkalinity," in *Water Quality*. Springer, 2015, pp. 153–178.

[82] S. Deekae, J. Abowei, and J. Alfred-Ockiya, "Seasonal variation of some physical and chemical parameters of luubara creek, ogoni land, niger delta, nigeria," *Research Journal of Environmental and Earth Sciences*, vol. 2, no. 4, pp. 208–215, 2010.

[83] P. N. Bande and S. Nandedkar, "Survey of water quality measurements sensors," *International Journal of research in Engineering and Technology*, vol. 5, no. 06, 2016.

[84] S. Pal, D. Das, and K. Chakraborty, "Colour optimization of the secchi disk and assessment of the water quality in consideration of light extinction coefficient of some selected water bodies at cooch behar, west bengal," *International Journal of Multidisciplinary Research and Development*, vol. 2, no. 3, pp. 513–518, 2015.

[85] E. T. Harvey, S. Kratzer, and P. Philipson, "Satellite-based water quality monitoring for improved spatial and temporal retrieval of chlorophyll-a in coastal waters," *Remote Sensing of Environment*, vol. 158, pp. 417–430, 2015.

[86] Y. Park, K. H. Cho, J. Park, S. M. Cha, and J. H. Kim, "Development of early-warning protocol for predicting chlorophyll-a concentration using machine learning models in freshwater and estuarine reservoirs, korea," *Science of the Total Environment*, vol. 502, pp. 31–41, 2015.

[87] P. De Wilde, "The gap between predicted and measured energy performance of buildings: A framework for investigation," *Automation in Construction*, vol. 41, pp. 40–49, 2014.

[88] F. Nie, J. Yuan, and H. Huang, "Optimal mean robust principal component analysis," in *International Conference on Machine Learning*, 2014, pp. 1062–1070.

[89] R. A. Johnson, D. W. Wichern *et al.*, *Applied multivariate statistical analysis*. Prentice-Hall New Jersey, 2014, vol. 4.

[90] H. Jarvie, B. Whitton, and C. Neal, "Nitrogen and phosphorus in east coast british rivers: speciation, sources and biological significance," *Science of the Total environment*, vol. 210, pp. 79–109, 1998.

[91] C. Christia, G. Giordani, and E. Papastergiadou, "Assessment of ecological quality of coastal lagoons with a combination of phytobenthic and water quality indices," *Marine pollution bulletin*, vol. 86, no. 1, pp. 411–423, 2014.

[92] R. Costanza, R. d'Arge, R. De Groot, S. Farber, M. Grasso, B. Hannon, K. Limburg, S. Naeem, R. V. O'neill, J. Paruelo *et al.*, "The value of the world's ecosystem services and natural capital," *nature*, vol. 387, no. 6630, pp. 253–260, 1997.

[93] I. Onyema and R. Popoola, "The physico-chemical characteristics, chlorophyll a levels and phytoplankton dynamics of the east mole area of the lagos harbour, lagos," *Journal of Asian Scientific Research*, vol. 3, no. 10, pp. 995–1010, 2013.

[94] S. Koponen, J. Pulliainen, K. Kallio, and M. Hallikainen, "Lake water quality classification with airborne hyperspectral spectrometer and simulated meris data," *Remote Sensing of Environment*, vol. 79, no. 1, pp. 51–59, 2002.

[95] X. Guan, J. Li, and W. G. Booty, "Monitoring lake simcoe water clarity using landsat-5 tm images," *Water resources management*, vol. 25, no. 8, pp. 2015–2033, 2011.

[96] C. Huang, J. Zou, Y. Li, H. Yang, K. Shi, J. Li, Y. Wang, X. Chena, and F. Zheng, "Assessment of nir-red algorithms for observation of chlorophyll-a in highly turbid inland waters in china," *ISPRS Journal of Photogrammetry and Remote Sensing*, vol. 93, pp. 29–39, 2014.

[97] S. Kay, J. D. Hedley, and S. Lavender, "Sun glint correction of high and low spatial resolution images of aquatic scenes: a review of methods for visible and near-infrared wavelengths," *Remote Sensing*, vol. 1, no. 4, pp. 697–730, 2009.

[98] F. L. Lobo, M. P. Costa, and E. M. Novo, "Time-series analysis of landsat-mss/tm/oli images over amazonian waters impacted by gold mining activities," *Remote Sensing of Environment*, vol. 157, pp. 170–184, 2015.

[99] J. G. Tundisi, M. A. Santos, and C. F. S. Menezes, "Tucuruí reservoir and hydroelectric power plant," *Sharing Experiences and Lessons Learned in Lake Basin Mangement, Burlington, Vermont. Management Experiences and Lessons Learned Brief*, vol. 1, pp. 1–20, 2003.

[100] P. Brezonik, K. D. Menken, and M. Bauer, "Landsat-based remote sensing of lake water quality characteristics, including chlorophyll and colored dissolved organic matter (cdom)," *Lake and Reservoir Management*, vol. 21, no. 4, pp. 373–382, 2005.

[101] N. T. T. Ha, K. Koike, and M. T. Nhuan, "Improved accuracy of chlorophyll-a concentration estimates from modis imagery using a two-band ratio algorithm and geostatistics: As applied to the monitoring of eutrophication processes over tien yen bay (northern vietnam)," *Remote Sensing*, vol. 6, no. 1, pp. 421–442, 2013.

[102] R. Doerffer, H. Schiller, J. Fischer, R. Preusker, and M. Bouvet, "The impact of sun glint on the retrieval of water parameters and possibilities for the correction of meris scenes," in *Proceedings of the 2nd MERIS/(A) ATSR User Workshop, ESA SP-666,(ESA, Frascati, Italy, 2008)*, 2008.

[103] E. J. Hochberg, S. Andrefouet, and M. R. Tyler, "Sea surface correction of high spatial resolution ikonos images to improve bottom mapping in near-shore environments," *IEEE transactions on geoscience and remote sensing*, vol. 41, no. 7, pp. 1724–1729, 2003.

[104] T. Kutser, E. Vahtmäe, and J. Praks, "A sun glint correction method for hyperspectral imagery containing areas with non-negligible water leaving nir signal," *Remote Sensing of Environment*, vol. 113, no. 10, pp. 2267–2274, 2009.

[105] H. Fukushima, M. Toratani, H. Murakami, P.-Y. Deschamps, R. Frouin, and A. Tanaka, "Evaluation of adeos-ii gli ocean color atmospheric correction using simbada handheld radiometer data," *Journal of oceanography*, vol. 63, no. 3, pp. 533–543, 2007.